

ECL Canada

Schlumberger

**SECTION 12-28 POOL STUDY
3D RESERVOIR MODELLING**

Version 2.0

February 8, 2005

Confidential



Proprietary Notice

Schlumberger Information Solutions, unpublished work, created 2003. These materials contain confidential, proprietary information and trade secrets of Schlumberger. All use, disclosure, and/or reproduction is prohibited unless authorized in writing. All rights reserved

Restricted Rights Legend

Use, duplication, or disclosure by the Government is subject to restrictions as set forth in subparagraph C(1)(ii) of the Rights in Technical Data and Computer Software clause at DFARS 252.277-7013.

SCHLUMBERGER INFORMATION SOLUTIONS

Disclaimer

The inclusion of any features described here is not a commitment to provide such features, now or in the future.

Project Manager:

Dana Coddling

Project Contact:

Dana Coddling

Author(s) (alphabetized):

Coddling, Dana
Nguyen, Hanh

Version Number	Date	Comments
0.1	1/24/2005	Draft report document
1.0	2/4/2005	Final report
2.0	2/8/2005	Final report

Trademarks

GeoQuest, GeoFrame, Petrel Workflow Tools, IESX, ELANPlus, Geology Office, Modeling Office are trademarks of Schlumberger Technology Corporation. Other product names are trademarks or registered trademarks of their respective holders.

Executive Summary

ECL Canada and Schlumberger SIS™ constructed three-dimensional geological models for the Section 12-28 pool. The available data includes structure maps and fluid zone boundary maps of the McMurray formation as well as log data for the 12-28 well and the wells in the Corner McMurray C pool. This small, one-section pool will be based entirely on the property distributions from the Corner C model. The objective of the study is to build a realistic model of geological facies distribution of the McMurray formation as well as other petrophysical properties associated with each of the geological facies.

A one-section grid consisting of 15,104 cells and with the dimensions of 100m x 100m x 1m in x, y and z directions was initialized. The McMurray formation was sub-divided into two zones: A1 sequence and the Lower McMurray. Facies distribution as well as petrophysical properties such as effective porosity PHIE, shale volume V_{sh} and fluid saturations were simulated using different geostatistical techniques where no well data were available. A summary of the simulation results for facies and other properties is given in the following tables.

Facies Code	Facies Name	Facies %	V_{sh} (mean)	Porosity (mean)	k_h (md) (mean)	k_v (md) (mean)	S_w (mean)*
0	Marine Mud	35.74	0.183	0.173	38.33	22.06	0.479
1	Marine Sand	10.35	0.024	0.310	505.71	443.64	0.461
2	Interbedded Mud	20.90	0.313	0.239	110.19	47.05	0.469
3	Sand	0.00	--	--	--	--	--
4	Breccia	0.00	--	--	--	--	--
5	Mud Plug	0.00	--	--	--	--	--
6	Limestone	0.00	--	--	--	--	--
7	Interbedded Sand	33.01	0.035	0.183	552.71	470.51	0.492
	Total	100					

Table 1: A1 Sequence summary statistics.

* S_w has cutoff of ≤ 0.75 applied

Facies Code	Facies Name	Facies %	V _{sh} (mean)	Porosity (mean)	k _h (md) (mean)	k _v (md) (mean)	S _w (mean)*
0	Marine Mud	6.76	0.275	0.170	55.78	15.31	0.396
1	Marine Sand	1.32	0.003	0.303	441.91	434.65	0.461
2	Interbedded Mud	18.98	0.254	0.271	103.28	27.53	0.288
3	Sand	42.24	0.086	0.336	1906.85	1364.20	0.236
4	Breccia	0.00	--	--	--	--	--
5	Mud Plug	7.93	0.468	0.209	7.28	1.21	0.339
6	Limestone	0.00	--	--	--	--	--
7	Interbedded Sand	22.77	0.077	0.284	167.75	131.46	0.471
	Total	100					

Table 2: Lower McMurray summary statistics.

* S_w has cutoff of <= 0.75 applied

Fluid saturations were created by incorporating information on fluid zone boundaries: gas, bitumen and water zones. Therefore, a combination of deterministic and geostatistical methods was applied for fluid saturation distribution.

Permeability was determined using different correlations. Horizontal permeability was calculated using a correlation between porosity and permeability, which is derived from available core analyses. Vertical permeability was calculated based on a correlation with V_{sh} and horizontal permeability.

Different scenarios or realizations were simulated for each property using geostatistical methods. All the realizations are equally probable. This situation occurs because geostatistics itself is a useful tool to assess uncertainty but not to replace it. With constraints in time and resources, only one realization for each property was chosen to represent the reservoir properties. Simple ranking techniques were developed for each property to process multiple realizations systematically. In a final result, one set of facies and petrophysical properties was selected and exported for reservoir flow simulation.

The final result from this study was transferred to a second grid suitable for the flow simulation study. The geological grid in this study was built at the simulation grid resolution, but a smaller grid around the well location was created at a much finer resolution of 1m by 50m by 1m.

The result of this study will be verified by the reservoir simulation study. If the geological model presented here is not a good description of the reservoir, then adjustments to the model should be made. Different property realizations can also be chosen to test different geological descriptions. New ranking techniques for multiple realizations may have to be developed to better guide the selection processes.

Contents

1.	Introduction	2
1.1.	Purpose	2
1.2.	Objectives.....	3
1.3.	Methodology.....	3
2.	Data Import and Editing.....	5
2.1.	Input data	5
3.	Structural Model	6
3.1.	Structure Maps	6
3.2.	3D Grids	6
3.3.	Upscaling of Well Logs.....	7
4.	Facies Modeling	8
4.1.	Statistical Analysis.....	8
4.2.	Variogram Analysis	13
4.3.	Simulation Results and Discussion.....	14
5.	Petrophysical Modeling	18
5.1.	Effective Porosity.....	18
5.1.1.	<i>Statistical Analysis</i>	<i>18</i>
5.1.2.	<i>Variogram Analysis.....</i>	<i>25</i>
5.1.3.	<i>Results and Discussion.....</i>	<i>26</i>
5.2.	Shale Volume (V_{sh}).....	28
5.2.1.	<i>Statistical Analysis</i>	<i>28</i>
5.2.2.	<i>Variogram Analysis.....</i>	<i>36</i>
5.2.3.	<i>Results and Discussion.....</i>	<i>36</i>
5.3.	Water Saturation (S_w).....	39
5.3.1.	<i>Statistical Analysis</i>	<i>39</i>
5.3.2.	<i>Zonation</i>	<i>47</i>
5.3.3.	<i>Variogram Analysis.....</i>	<i>49</i>
5.3.4.	<i>Results and Discussion.....</i>	<i>49</i>
5.4.	Horizontal Permeability	53
5.5.	Vertical Permeability	55
6.	Upscaling for Simulation.....	60
6.1.	Well-specific Simulation Grid	60
6.2.	Upscaling of properties	61
6.2.1.	<i>Small Grid Properties.....</i>	<i>61</i>
7.	Export	66
7.1.	Export format.....	66
8.	References	67

1. Introduction

1.1. Purpose

The purpose of this project is to construct 3D geological models for the Section 12-28 pool located at the Fort McMurray area. The location map of the pool is shown in Figure 1. The focus of the project is the McMurray formation, which has oil sands and shallow gas recovery potential. The study commenced in November 2004 in Calgary, Alberta.

The modeling was undertaken in Petrel Workflow Tools, a Schlumberger Information Solutions product.

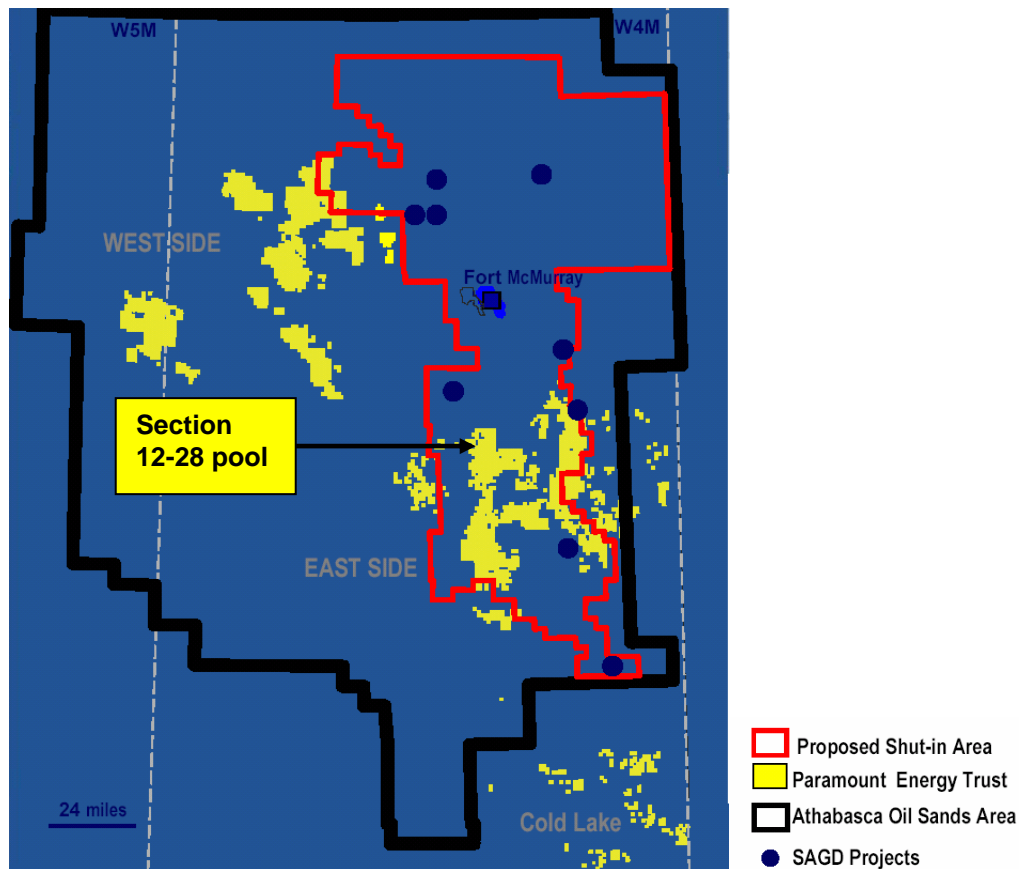


Figure 1: General Location Map

1.2. Objectives

The objectives of the study are:

- Build a 3D geological model for the entire pool at a coarser scale.
- Build 3D models at finer grids that can be extracted and imported into flow simulation at selected reservoir locations suitable for SAGD recovery methods.
- Reservoir properties to be modelled are lithological facies, porosity, permeability, fluid saturations and shale volumes.

1.3. Methodology

Petrel Workflow Tools permits asset teams to perform modeling projects centered on a single software system. Petrel eliminates the need for data transfer and complex updating through multiple applications. It covers the entire workflow from data loading and quality control through to upscaling for simulation.

The workflow for this project was as follows:

1. Loading of well locations, logs, and structural surfaces.
 2. Editing and quality checking of input data.
 3. Structural modeling of 3D grid.
 4. Upscaling of well logs into structural 3D grid.
 5. Variogram modeling for all properties.
 6. Generation of 5 facies models and selection of one model for ongoing work.
 7. Generation of 5 porosity models biased to the chosen facies model, and selection of one model for ongoing work.
 8. Generation of 5 shale volume models biased to facies and collocated to the chosen porosity model, and selection of one model for ongoing work.
 9. Generation of 5 water saturation models biased to facies and collocated to the chosen porosity model, and selection of one model for ongoing work. Creation of gas saturation and bitumen saturation models based on fluid zones and water saturation.
 10. Generation of calculated horizontal permeability based on the chosen porosity model.
 11. Generation of calculated vertical permeability based on the horizontal permeability and the shale volume property.
-

12. Creation of several simulation grids, including a large coarse grid covering the entire project area and small grids around each well location.
13. Export of grids for simulation in CMG.

2. Data Import and Editing

2.1. Input data

The input data was provided by Paramount Energy Trust and/or its contractors.

The data for this study consists of single elevation values for the three surfaces (Paleozoic, Base of A1sequence and top of McMurray) and log data for the 12-28 well (Table 3). A plot of well locations is shown in Figure 2. Paramount and/or its independent contractors provided petrophysical and geological analysis of log data.

Log data consists of conventional suites of logs such as GR, SP, porosity, and resistivity curves. Interpreted curves are effective porosity PHIE, shale volume V_{sh} , water saturation S_w , lithological facies and permeability. Fluid level (gas, water, bitumen) and stratigraphic picks based on log data were also available.

UWI	Short Name	KB	X	Y
12-28-081-10	12-28	705.7	467989.94	6211793.09

Table 3: Well location data for the Section 12-28 Pool

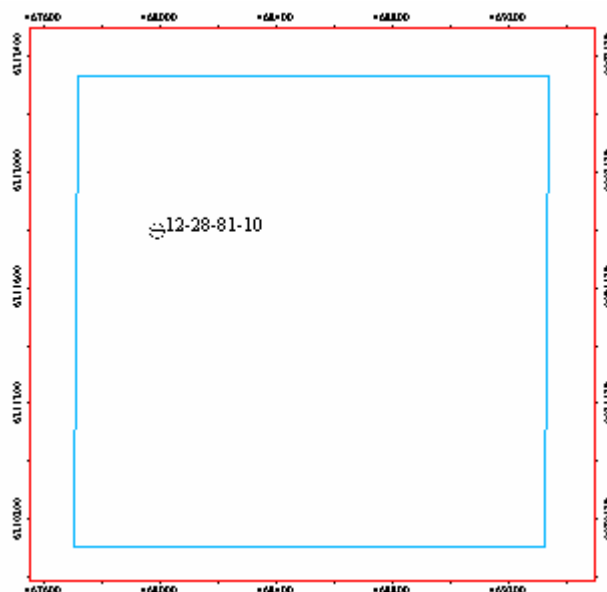


Figure 2: Location Map for wells in Section 12-28

3. Structural Model

Before distributing properties, a structural grid must be created. Petrel's grid building routines (Pillar Gridding, Make Horizons, Make Zones, and Layering) are designed to create an accurate faulted or unfaulted grid.

3.1. Structure Maps

Single elevation values were given for each surface within the section. These single values were gridded into flat surfaces at that given elevation (Table 4).

Well	Paleozoic	A1_Base	McMurray
12-28	224.95	281.7	282.45

Table 4: Stratigraphic interpretations (TVDSS m)

3.2. 3D Grids

In the horizontal directions X and Y, the reservoir was divided into a 100m x 100m grid. Figure 3 shows the areal view of the 3D grid. The formations above the McMurray top and below the Paleozoic unconformity were excluded from the model. The reason for this exclusion is because the main focus of this study is the McMurray formation. A smaller number of cells in the model will speed up the simulation process.

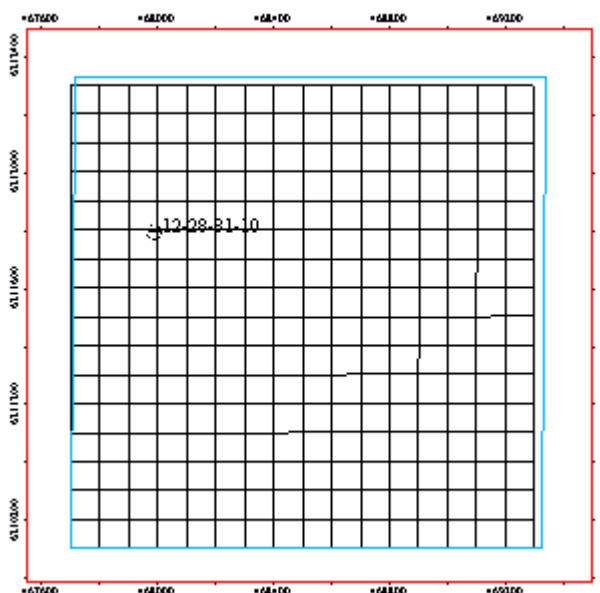


Figure 3: Areal gridding for the 3D grid – 100m by 100m

The McMurray formation subsequently was divided into two sequences. The first one is from the McMurray top to the base of A1 sequence. The second one is from the A1 base to the Paleozoic unconformity. The upper sequence is called the A1 sequence; the lower sequence is called the lower McMurray in this report.

The A1 sequence was divided into two layers. The lower McMurray was divided into layers with 1m thickness and parallel to the Paleozoic base. Since the bounding horizons are flat surfaces, the cells parallel to both the top and base horizons of the zone.

The 3D grid has 16, 16 and 59 cells in X, Y and Z directions, respectively. The total number of cells in the 3D grid is 15,104 cells.

3.3. Upscaling of Well Logs

The structural grid consists of a matrix of cells. Each grid cell has a single value for each property, e.g. Facies. As the grid cells are often much larger than the sample density for the well logs, the well log data must be scaled up or blocked before they can be entered into the grid.

When scaling up the well logs, Petrel will first find all the 3D grid cells the wells penetrate. For each of these penetrated cells, all well log values that fall within the bounds of the cell will be averaged according to a user-selected algorithm to produce one value for that cell. This is standard operating procedure in all geomodeling software packages.

Property Type	Upscaling Algorithm used
Facies	Most Appearing Facies
Porosity	Arithmetic
Shale volume	Arithmetic
Water saturation	Arithmetic

Table 5: Upscaling algorithms used

4. Facies Modeling

The facies property will be distributed first, and will be used to guide the distributions of other properties – shale volumes, porosity, and water saturation.

4.1. Statistical Analysis

Lithological facies were given to ECL Canada and Schlumberger SIS™ by Paramount and/or its independent contractors as one of the properties in the log data. The assignment of the facies at each logging interval was possible using discriminant analysis. A separate report will provide more detailed information about this facies analysis for the Section 12-28 pool.

There are 8 facies identified for the formations of interest in the surrounding area. These facies were coded as numbers before importing into the model.

Code	Facies Type
0	Marine Mud
1	Marine Sand
2	Interbedded Mud
3	Sand
4	Breccia
5	Mud Plug
6	Limestone
7	Interbedded Sand

Table 6: Facies coding for import

Facies data from logs were upscaled into the 3D grid, because the log resolution is greater than the 3D grid resolution (log intervals are about 0.2 m per reading while the cell size in the Z direction is about 1 m). The facies that occur most in logs during the 1 m interval will be assigned to the cell center.

Due to the limitation of the available data for this pool, the facies proportion derived from the one well within the pool boundary was not representative for the area. In order to solve this issue, facies proportions and variogram models were taken from the C McMurray pool and incorporated into this single well pool.

The 11 Corner C wells were moved into the 12-28 section by editing their X and Y positions in Petrel. They were upscaled into the Section 12-28 pool grid and used together with the 12-28 well to generate vertical proportion curves for facies modeling. However, only the 12-28 well facies data was used as input for the actual simulation of facies, so a second pass of Scale Up Well Logs was run to eliminate the wells from the Corner C pool. In the final

results, the proportion curves from the Corner C and 12-28 wells were kept. Also, only facies data input from the 12-28 well was retained.

In the McMurray formation, limestone is absent. Breccia, although present in the well logs, was not present in the upscaled log data due to its relative thinness when compared with the thickness of the cells. The “most of” algorithm did not carry through the Breccia cells as they were never the most significant portion of any one-meter interval.

Figure 4, Figure 5 and Table 7 compare relative facies proportions between original and upscaled log data for the two sub-sequences of the McMurray. These facies proportions were calculated from the combination of the 12-28 well and the Corner C wells. It can be observed that the relative facies proportions are very close between the original and upscaled logs.

Code	Facies Names	A1 Sequence		Lower McMurray	
		Raw Log %	Upscaled %	Raw Log %	Upscaled %
0	Marine Mud	75	70.00	7.1	7.37
1	Marine Sand	5	10.00	2.5	1.05
2	Interbedded Mud	10	10.00	17.3	20.00
3	Sand	0	0.00	41.5	40.70
4	Breccia	0	0.00	0.5	0.00
5	Mud Plug	0	0.00	8.9	7.02
6	Limestone	0	0.00	0	0.00
7	Interbedded Sand	10	10.00	22.2	23.86
Total		100	100	100	100

Table 7: Facies proportions calculated from combination of 12-28 well and Corner C wells

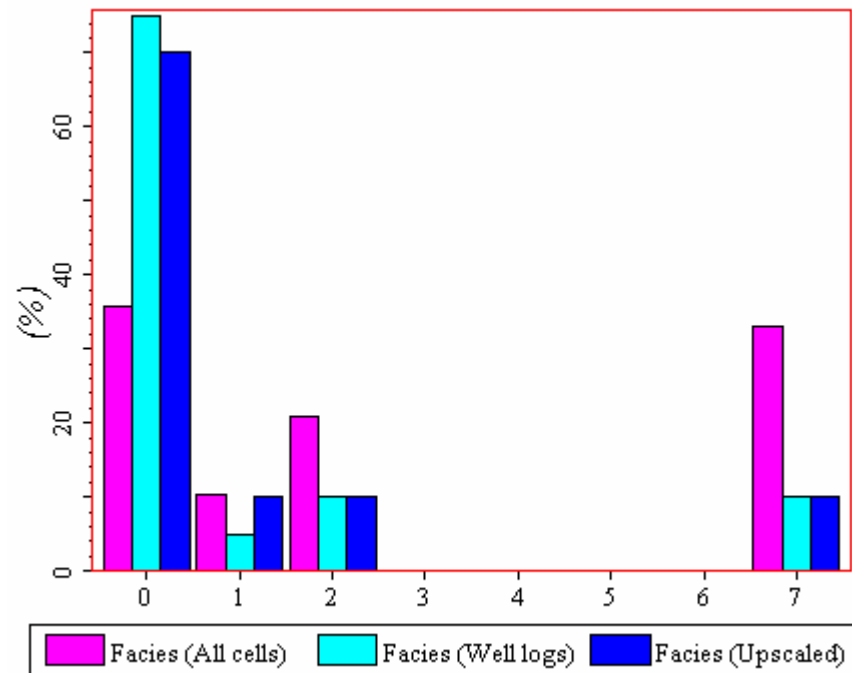


Figure 4: Facies Proportions from original and upscaled logs - A1 sequence

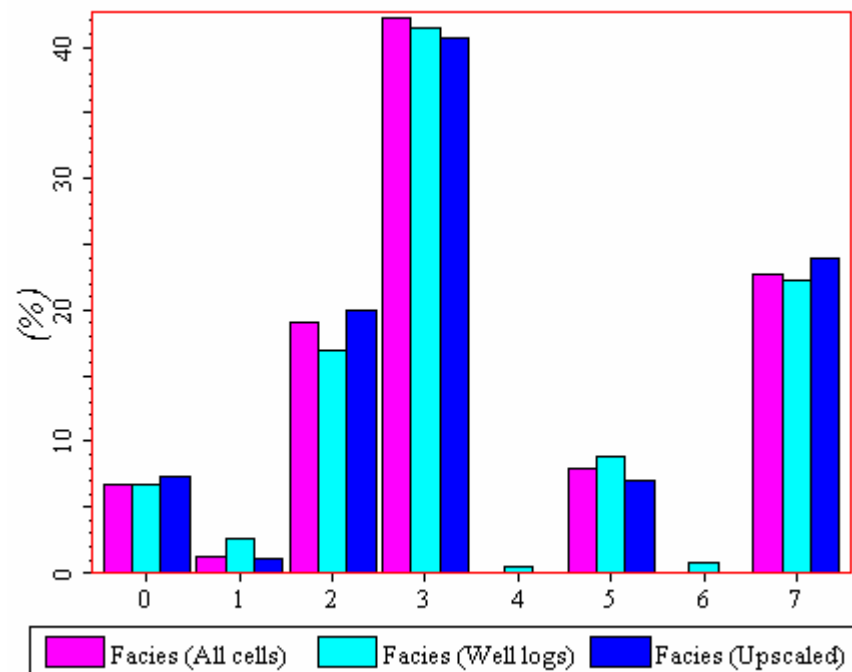


Figure 5: Facies proportion from original and upscaled logs - Lower McMurray

Facies distribution is different in the upper and lower parts of the McMurray. In the upper A1 sequence, there are only 4 facies present: Marine Mud, Marine Sand, Interbedded Mud and Interbedded Sand. In other words, marine facies are dominant. In the lower part of the McMurray, although all 7 facies are present, 3 facies Interbedded Mud, Interbedded Sand and Sand are the three dominant facies among all the facies.

Figure 7 and Figure 8 show the facies proportion by layer in the McMurray formation. In the A1 sequence, the vertical facies proportion was manually edited to better describe the facies relative proportion. Therefore, the global facies histogram in the A1 sequence will be different from the input log data. In the Lower McMurray part, the facies proportions were preserved from the log input data (combined sources). Sand and Interbedded Sand are the predominant facies at the lower part of the formation. This facies proportion by layer and the global proportion presented in the facies histogram will be used as constraints during the 3D stochastic facies distribution simulation.



Figure 6: Facies legend

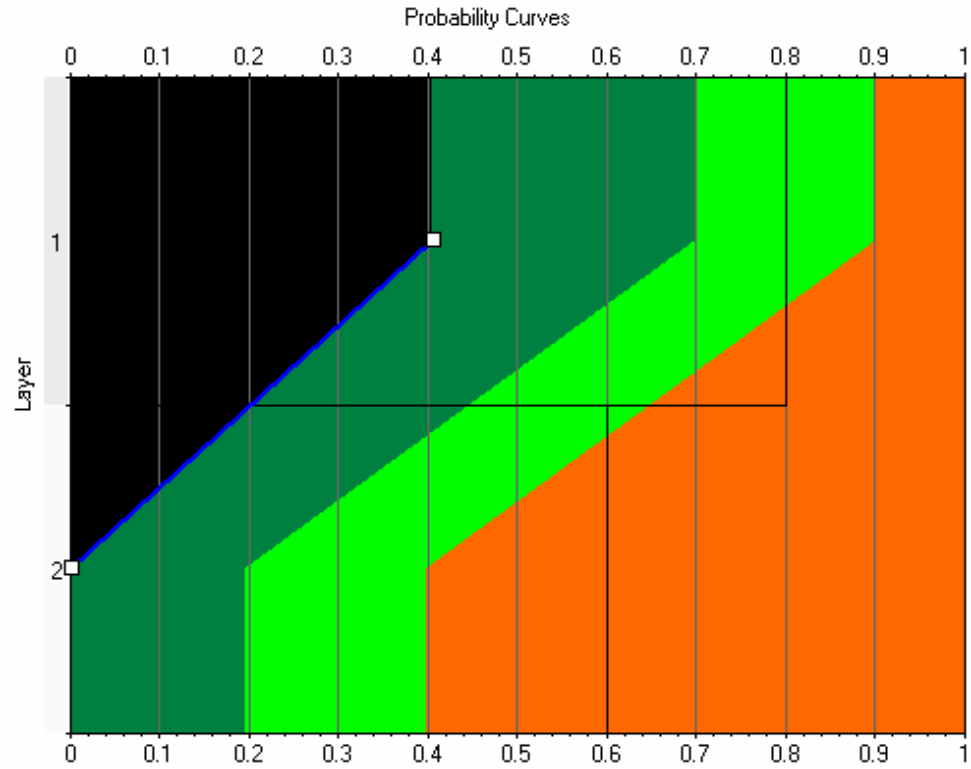


Figure 7: Vertical facies proportions – Upscaled logs, A1 sequence

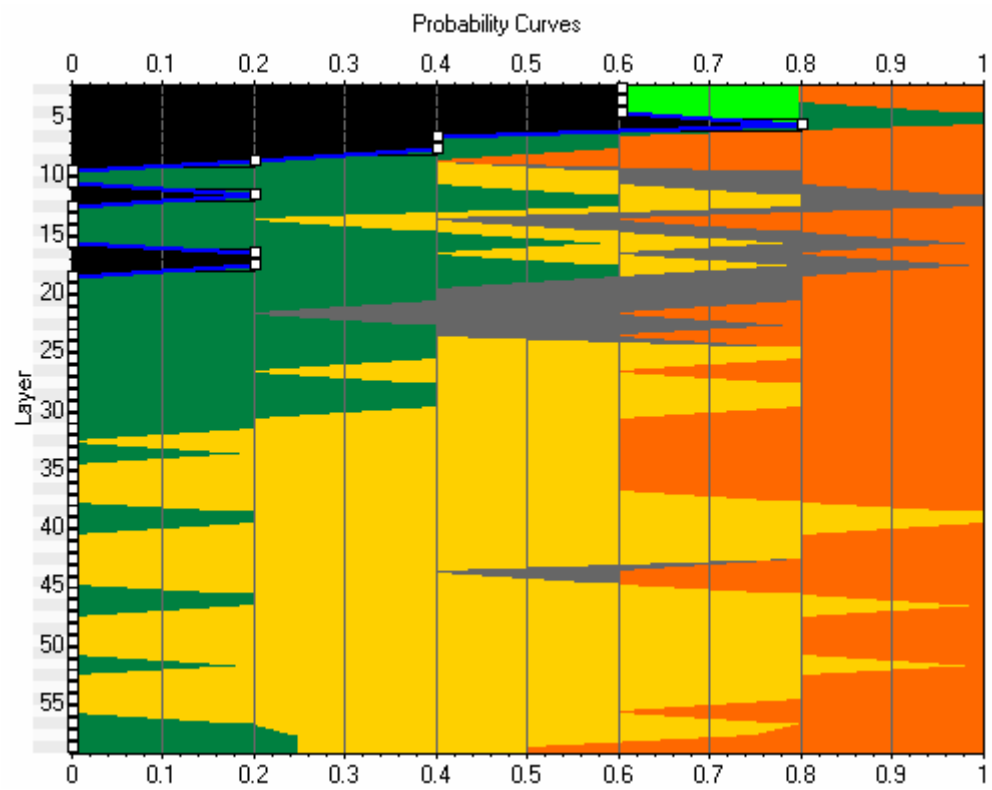


Figure 8: Vertical facies proportions – Upscaled logs, Lower McMurray

4.2. Variogram Analysis

Definition of variograms and other geostatistical terms can be found in any standard geostatistical textbooks [1,2,3]. In short, a variogram is a measure of the spatial continuity of any geological property. Experimental variograms are calculated from the sample data (logs, cores, seismic...). Variogram models, on the other hand, have a strict mathematical definition. For a specific geological property, a variogram model that best fits the experimental variogram is used for stochastic simulation. Many times, a few variogram models are used at the same time (nested structures) to better fit the experimental variograms.

It should be mention that experimental variograms from sample data are not always perfectly fit with the variogram models. It can happen if the number of data samples is limited or the data quality is low. In this situation, experimental variogram can look noisy. Additional geological information is required to better define variogram model parameters.

The facies variogram parameters for the Section 12-28 pool (Table 8 and Table 9) are taken directly from variogram models of the Corner McMurray C pool. This is because of the limitation in the data available, as explained above.

Facies	Nugget	Type	Anisotropy Angle	Ranges (m)		
				Major	Minor	Vertical
Marine Mud	0.146	Exponential	0	1000	1000	1.5
Marine Sand	0.2	Exponential	0	1000	1000	2.5
Interbedded Mud	0.146	Exponential	0	500	500	1.6
Interbedded Sand	0.146	Exponential	0	500	500	1.9

Table 8: Variogram Models for A1 Sequence

Facies	Nugget	Type	Anisotropy Angle	Ranges (m)		
				Major	Minor	Vertical
Marine Mud	0.146	Exponential	0	1000	1000	2.3
Marine Sand	0.073	Exponential	0	1000	1000	3.8
Interbedded Mud	0.146	Exponential	0	500	500	4.3
Sand	0.146	Exponential	0	1000	500	7.2
Mud Plug	0.061	Exponential	0	200	200	3.3
Interbedded Sand	0.047	Exponential	0	500	500	2.7

Table 9: Variogram Models for Lower McMurray

4.3. Simulation Results and Discussion

Sequential Indicator Simulation (SIS) was used to populate the facies for the McMurray formation. Facies simulation for the A1 sequence and Lower McMurray was done separately. A simple kriging type was applied in simulation parameter setting. Five realizations of facies were generated, of which only one facies realization was chosen for further petrophysical properties modelling.

Statistics on facies distribution for different realizations is given in Table 10 and Table 11. For the A1 sequence, the facies proportions vary significantly from realization to realization. It may be due to the fact that the number of cells belonging to the A sequence is very small. For the Lower McMurray sequence, all the facies realizations have very similar facies proportion. Therefore, it is difficult to determine a quantitative method of ranking facies realizations. In this study, since the realizations had similar input data, the midpoint realization was chosen by visual inspection by Paramount and Schlumberger staff. The realization chosen was #5.

A 3D view of the facies distribution from realization 5 is shown in Figure 9. Facies distribution along a north-south cross-section through the well 12-28 is shown in Figure 10.

Code	Name	R1 %	R2 %	R3 %	R4 %	R5 %
0	Marine Mud	28.91	44.73	28.91	46.09	35.74
1	Marine Sand	19.73	15.63	16.60	6.45	10.35
2	Interbedded Mud	24.22	10.16	16.80	16.02	20.90
7	Interbedded Sand	27.15	29.49	37.70	31.45	33.01
	Total	100	100	100	100	100

Table 10: Facies Distribution for 5 Simulation Realizations, A1 Sequence

Code	Name	Upscaled %	R1 %	R2 %	R3 %	R4 %	R5 %
0	Marine Mud	7.37	6.85	6.56	6.62	6.02	6.76
1	Marine Sand	1.05	0.87	1.45	0.70	1.73	1.32
2	Interbedded Mud	20.00	21.21	22.09	21.78	23.55	18.98
3	Sand	40.70	38.91	38.86	40.52	39.95	42.24
4	Breccia	0.00	0.00	0.00	0.00	0.00	0.00
5	Mud Plug	7.02	7.07	8.05	7.93	7.34	7.93
6	Limestone	0.00	0.00	0.00	0.00	0.00	0.00
7	Interbedded Sand	23.86	25.09	22.99	22.45	21.41	22.77
	Total	100	100	100	100	100	100

Table 11: Facies Distribution for 5 Simulation Realizations, Lower McMurray

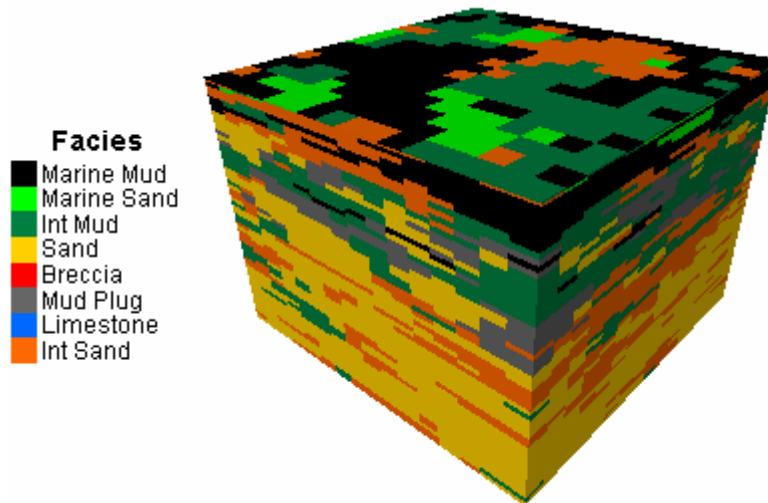


Figure 9: 3D view of Facies realization #5

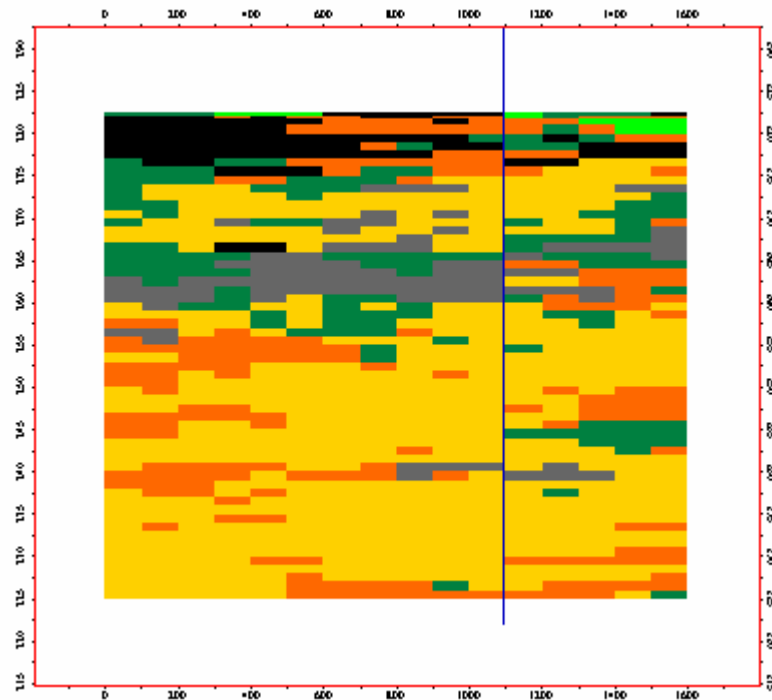


Figure 10: North-South cross-section line through Facies realization #5 and well 12-28

Vertical facies proportion (by layers) for realization 5 is shown in Figure 11 and Figure 12. As it can be observed, the vertical facies proportion is preserved. The vertical facies proportion profile from simulation is smoother compared with the constrained one from the original logs though. Thinner beds in the facies vertical proportion calculated from the original log data are averaged or lost. This is a direct result of the grid resolution in the vertical direction. Fine log resolution was partially lost during the log upscaling

process. As the result, the facies vertical distribution from the simulation is smoother.

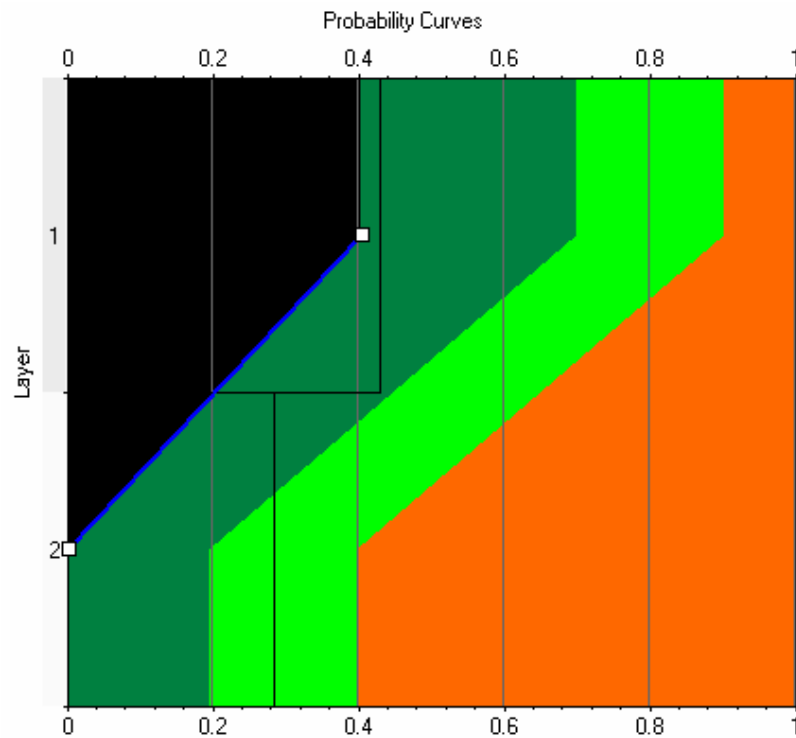


Figure 11: Vertical facies proportions - simulated data, A1 sequence

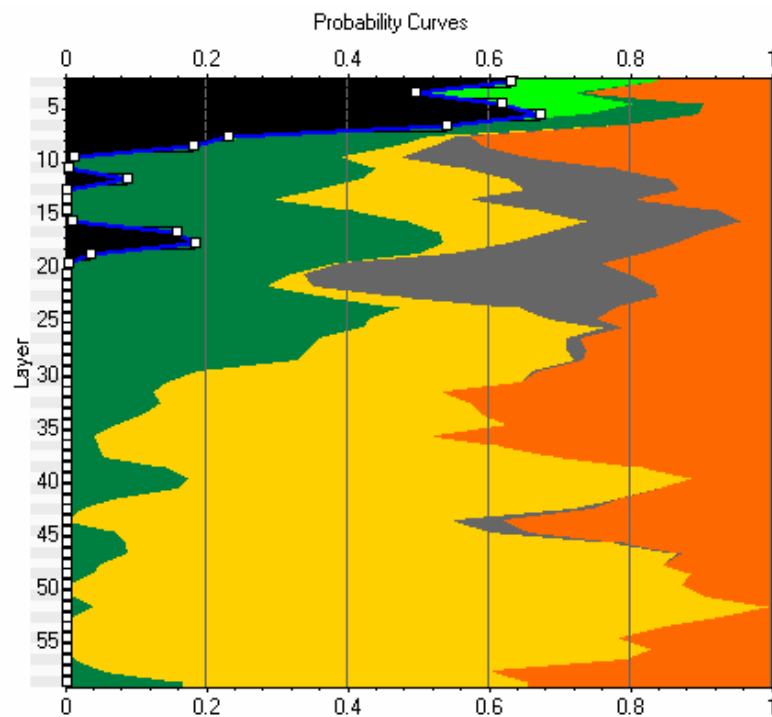


Figure 12: Vertical facies proportions - simulated data, Lower McMurray

Comparisons of facies distributions between original log data and simulation is shown in Figure 13 and Figure 14.

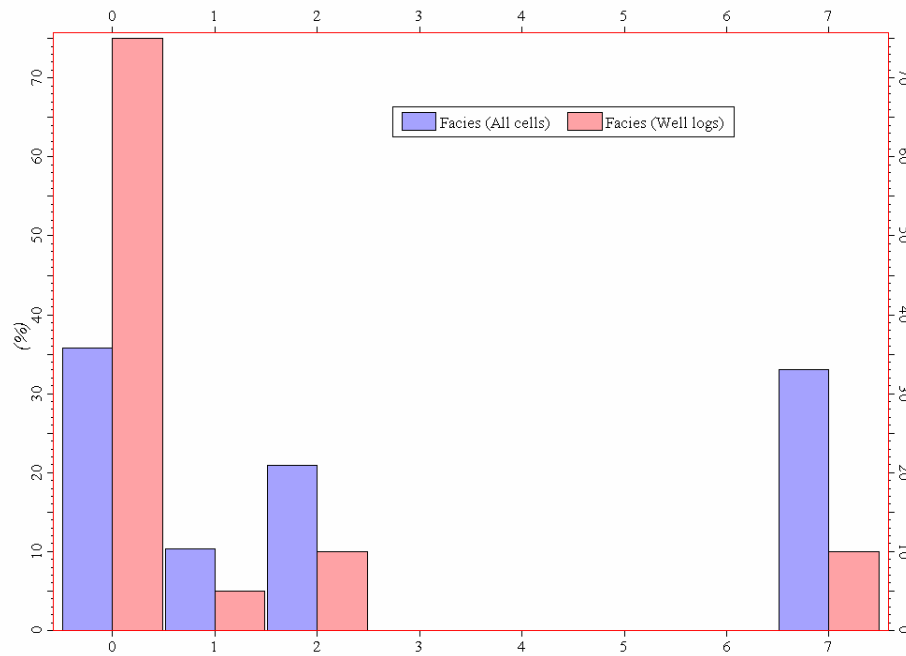


Figure 13: Comparison of facies distribution #5 and raw logs, A1 Sequence

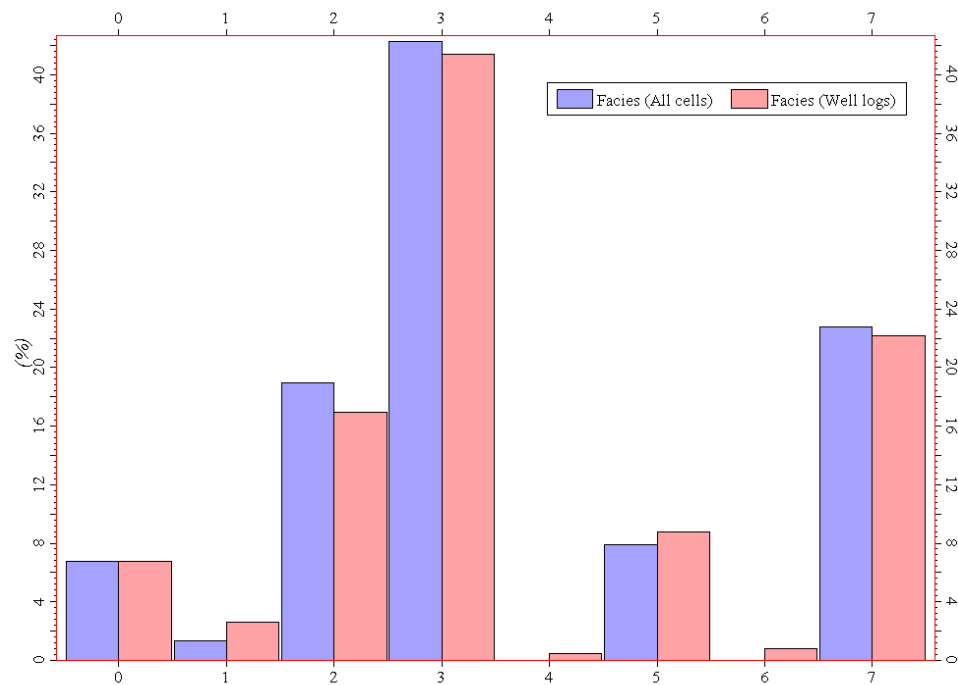


Figure 14: Comparison of facies distribution #5 and raw logs, Lower McMurray

5. Petrophysical Modeling

The following petrophysical properties will be modeled:

- Effective porosity PHIE
- Shale volume V_{sh}
- Horizontal Permeability k_h
- Vertical Permeability k_v
- Saturation: water, gas and bitumen S_w , S_g , S_o

5.1. Effective Porosity

5.1.1. Statistical Analysis

In the Section 12-28 pool, the Mud Plug and Marine Mud facies had significant porosity and shale volume values. Therefore, PHIE for those two mud facies will be simulated using geostatistical methods. Since there is limitation in data available (only one well in the pool boundary), PHIE statistics for some facies is not reliable. Therefore, some statistics for the PHIE simulation such as PHIE minimum, maximum, mean, and standard deviation have to be taken from the analogue Corner McMurray C pool. Table 12 and Table 13 below list basic PHIE statistical information for different facies that have more reliable statistics data. Table 14 and Table 15 list basic input statistics for PHIE taken from the Corner McMurray C pool.

Facies	PHIE Original Logs			PHIE upscaled Logs		
	Min	Max	Mean	Min	Max	Mean
Marine Mud	0.231	0.277	0.253	0.264	0.264	0.264
Marine Sand	--	--	--	--	--	--
Interbedded Mud	--	--	--	--	--	--
Interbedded Sand	0.302	0.399	0.322	0.328	0.328	0.328

Table 12: Basic Statistics of PHIE for Different Facies-Original and Upscaled Logs, A1 Sequence

Facies	PHIE Original Logs			PHIE upscaled Logs		
	Min	Max	Mean	Min	Max	Mean
Marine Mud	0.267	0.281	0.273	0.273	0.273	0.273
Marine Sand	--	--	--	--	--	--
Interbedded Mud	0.198	0.319	0.273	0.255	0.284	0.269
Sand	0.195	0.385	0.337	0.283	0.363	0.337
Mud Plug	0.173	0.236	0.208	0.192	0.221	0.208
Interbedded Sand	0.090	0.344	0.284	0.269	0.299	0.286

Table 13: Basic Statistics of PHIE for Different Facies-Original and Upscaled Logs, Lower McMurray

Facies	Min	Max	Mean	Standard Deviation
Marine Sand	0.2792	0.3368	0.3082	0.021
Interbedded Mud	0.0699	0.3129	0.2125	0.0918

Table 14: Additional Statistics for PHIE taken from Corner McMurray C pool, A1

Facies	Min	Max	Mean	Standard Deviation
Marine Sand	0.2655	0.3468	0.301	0.0209

Table 15: Additional Statistics for PHIE taken from Corner McMurray C pool, Lower McMurray

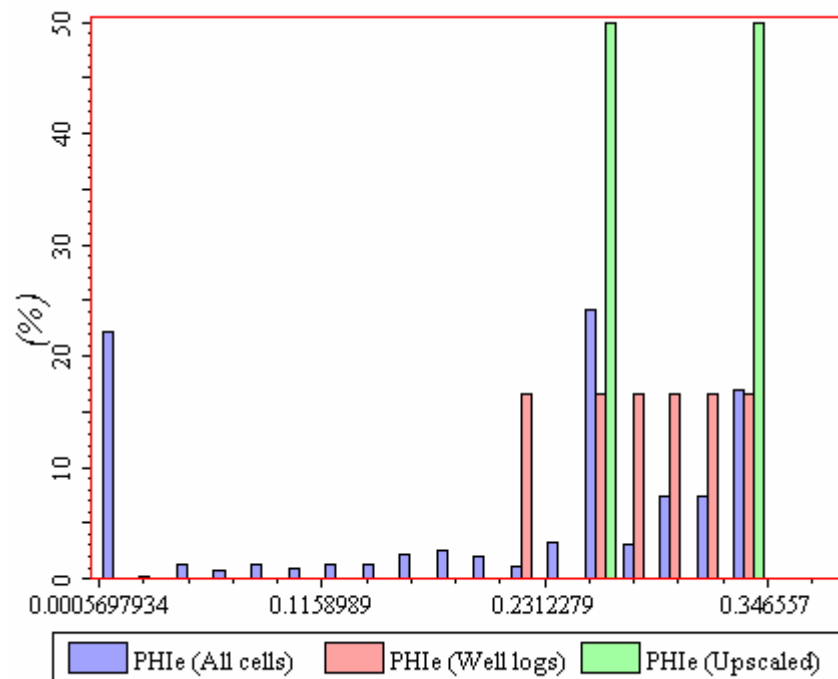


Figure 15: Upscaled and distributed values for porosity - A1sequence all facies

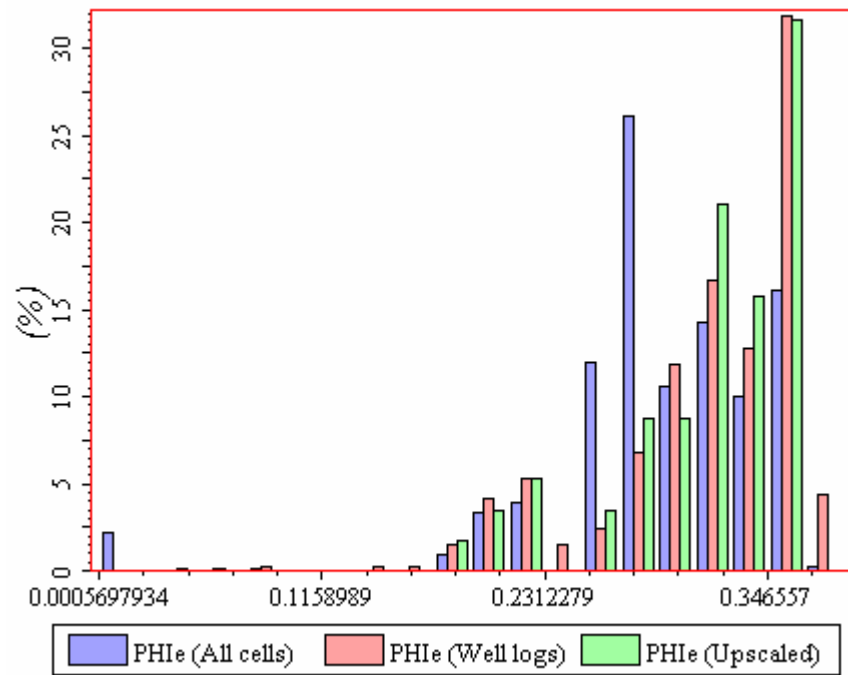


Figure 16: Upscaled and distributed values for porosity – Lower McMurray all facies

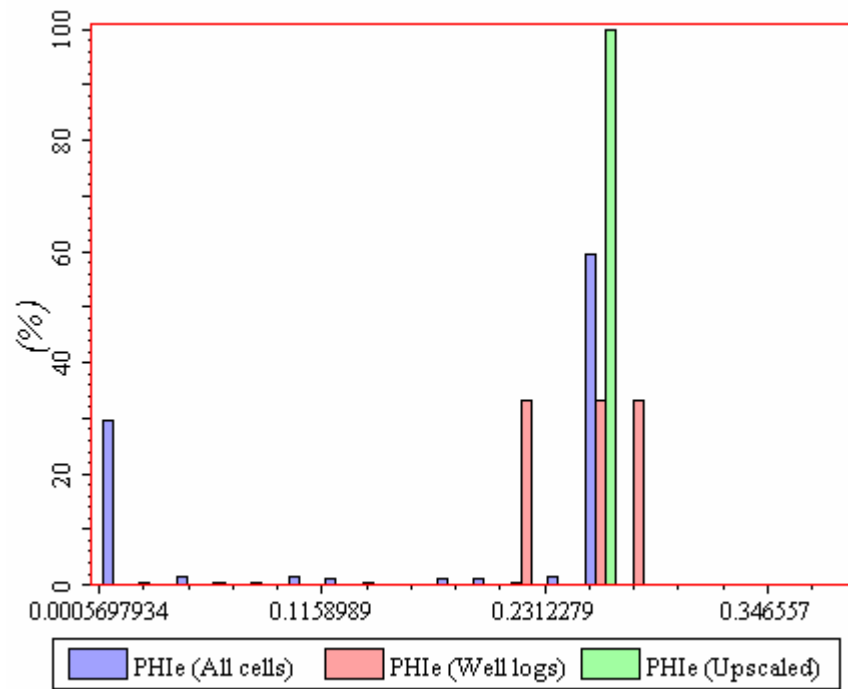


Figure 17: A1 Marine Mud Porosity

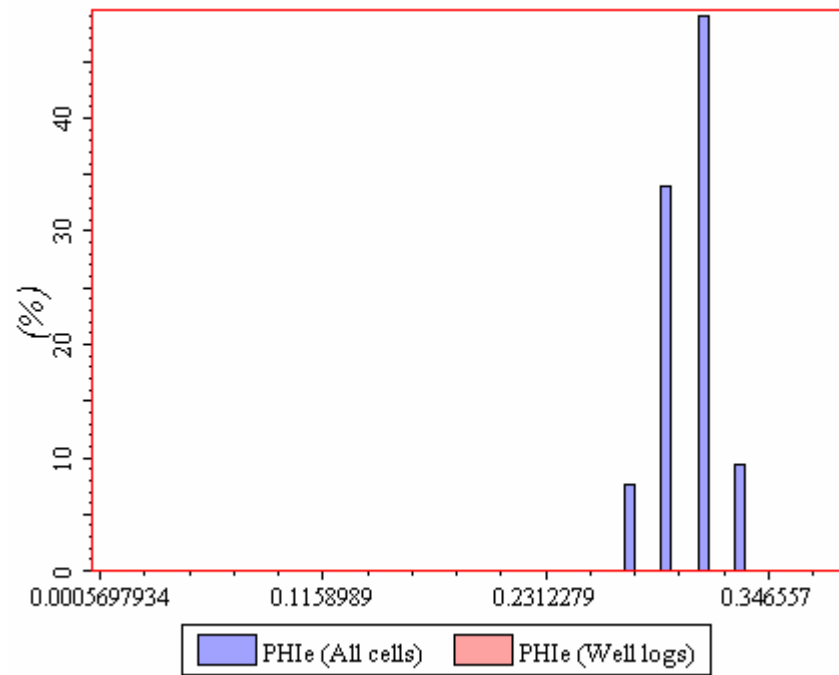


Figure 18: A1 Marine Sand Porosity

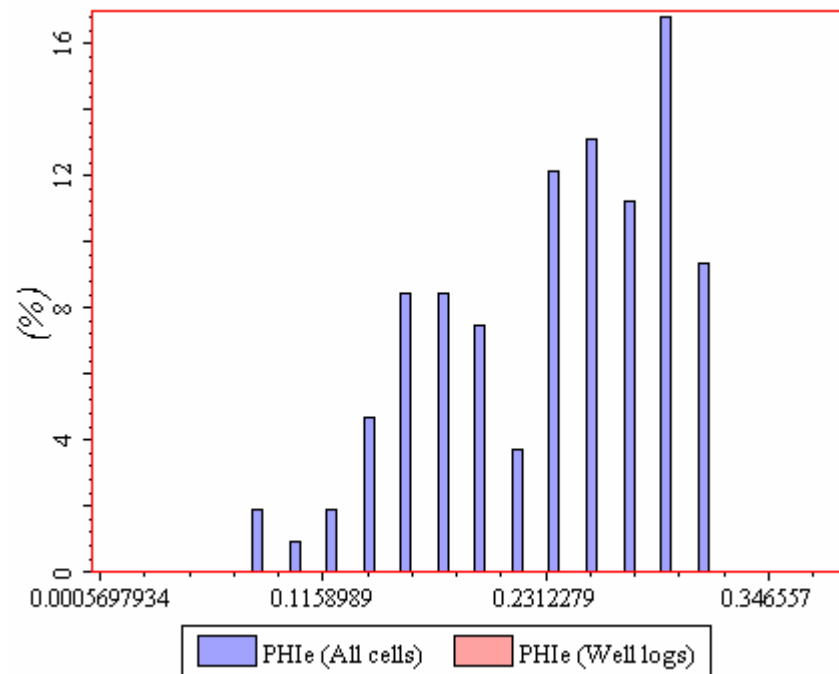


Figure 19: A1 Interbedded Mud Porosity

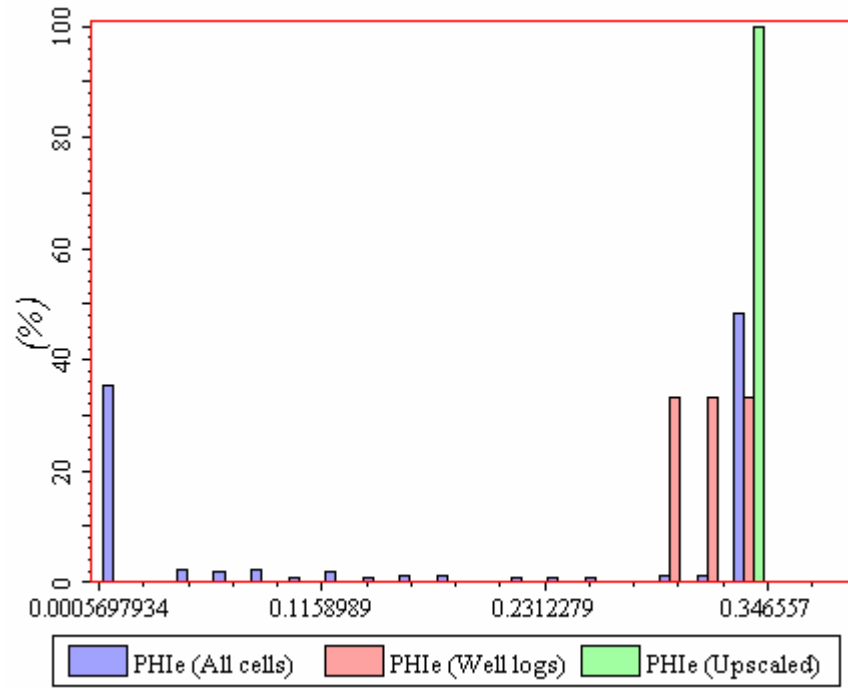


Figure 20: A1 Interbedded Sand Porosity

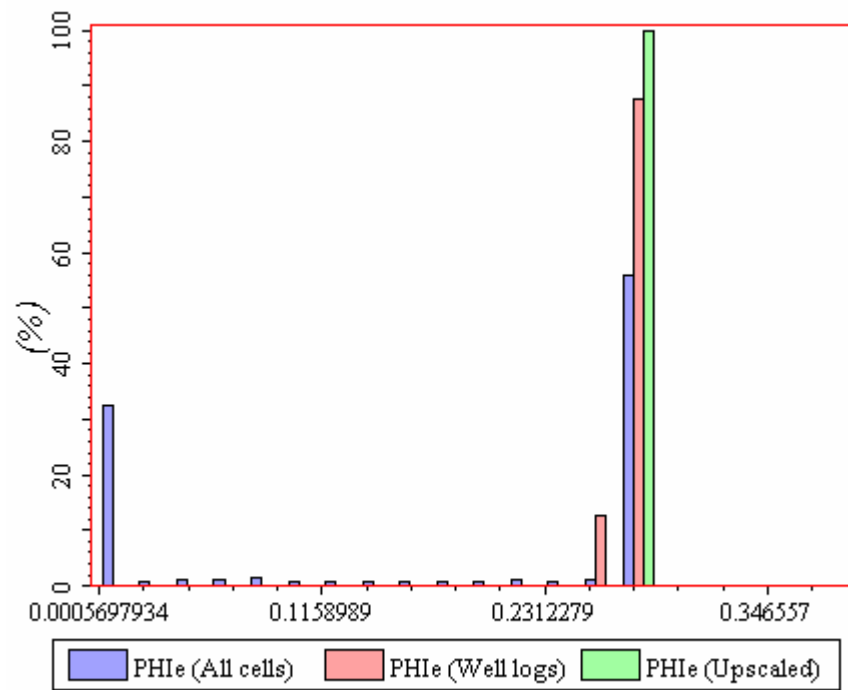


Figure 21: Lower McMurray Marine Mud Porosity

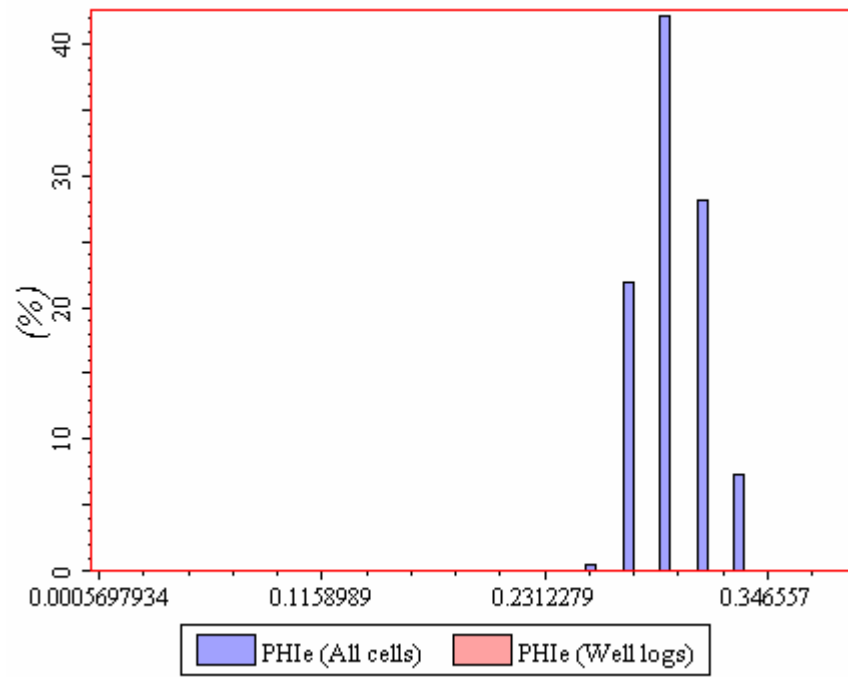


Figure 22: Lower McMurray Marine Sand Porosity

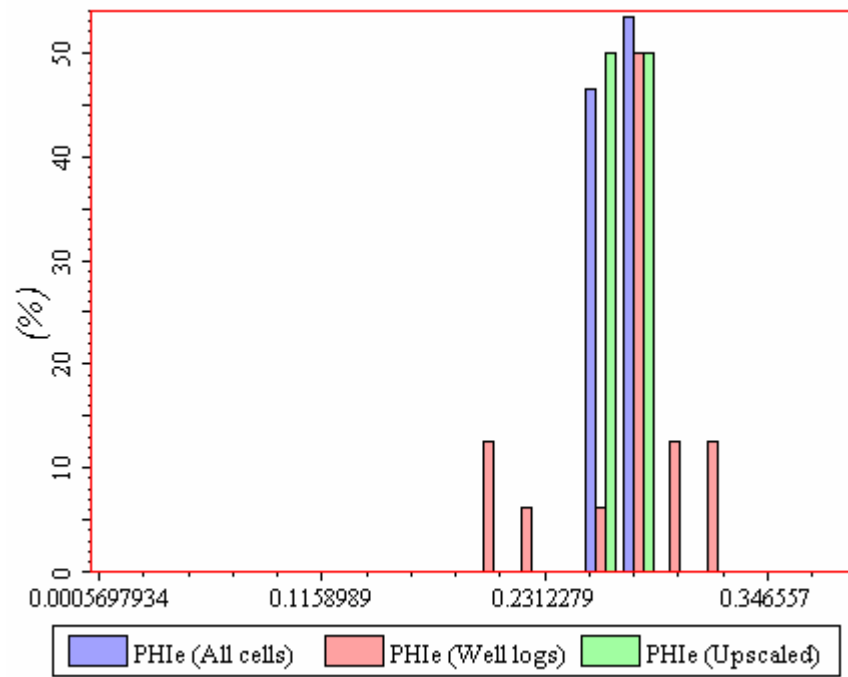


Figure 23: Lower McMurray Interbedded Mud Porosity

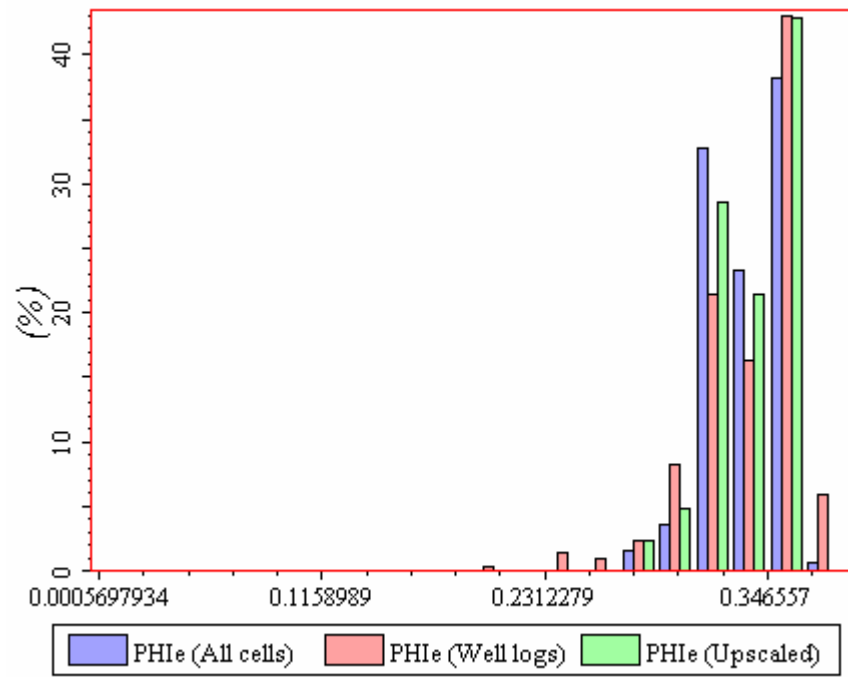


Figure 24: Lower McMurray Sand Porosity

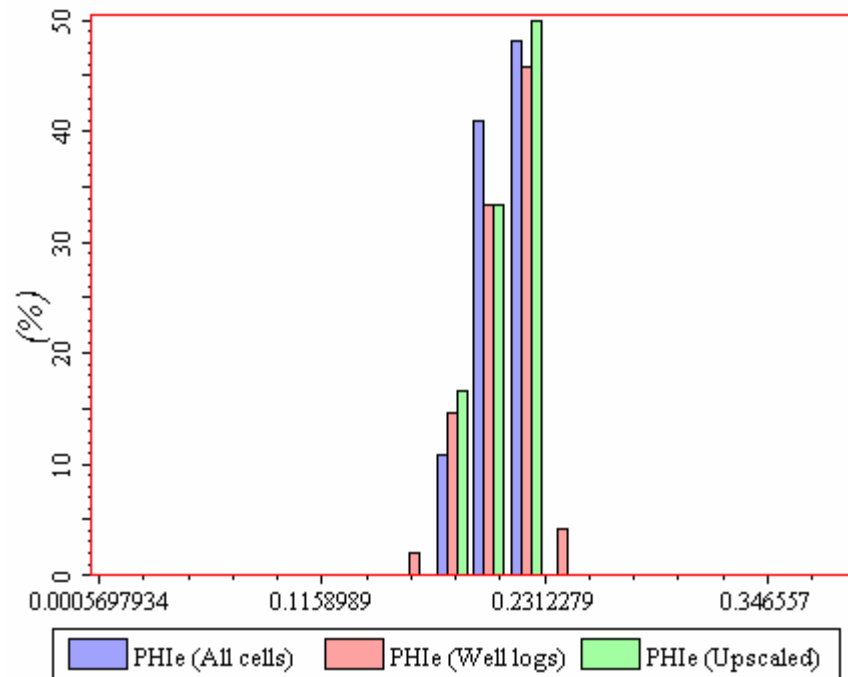


Figure 25: Lower McMurray Mud Plug Porosity

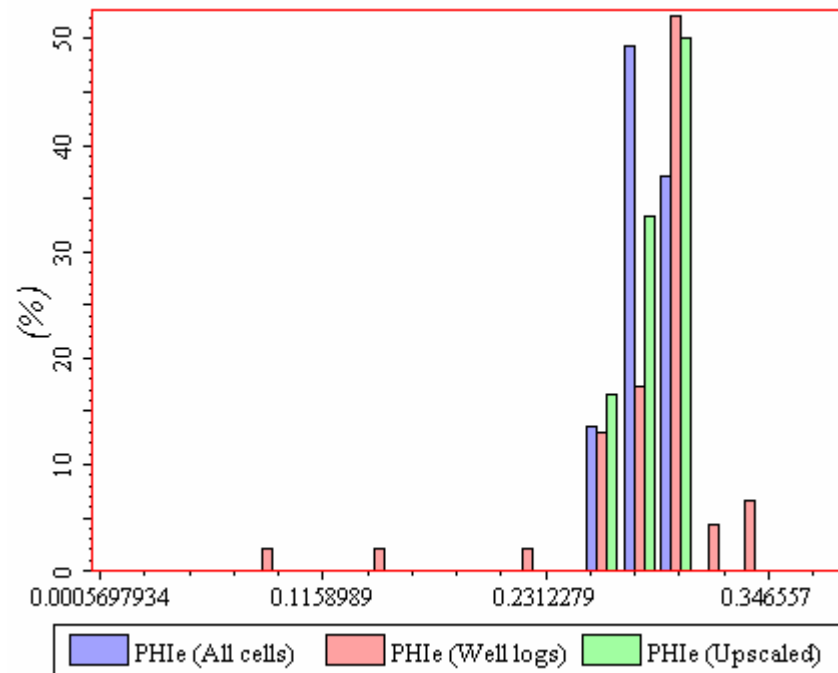


Figure 26: Lower McMurray Interbedded Sand Porosity

5.1.2. Variogram Analysis

Variograms for PHIE by facies were taken directly from the Corner C model. Table 16 and Table 17 tabulate variogram models applied for PHIE. More information on the variogram plots for different facies can be found in a similar report for the Corner C pool.

Facies	Nugget	Type	Anisotropy Angle	Ranges (m)		
				Major	Minor	Vertical
Marine Mud	0.2	Exponential	0	1000	1000	5.6
Marine Sand	0.072	Exponential	292	1000	1000	3.3
Interbedded Mud	0.067	Spherical	0	500	500	2.8
Interbedded Sand	0.2	Spherical	0	860	860	2.4

Table 16: PHIE Variogram Models, A1 Sequence, taken from the Corner C pool.

Facies	Nugget	Type	Anisotropy Angle	Ranges (m)		
				Major	Minor	Vertical
Marine Mud	0.2	Spherical	0	1000	1000	5.6
Marine Sand	0.072	Exponential	0	1000	1000	3.31
Interbedded Mud	0.067	Exponential	0	500	500	4.3
Sand	0.197	Spherical	323	1000	500	17.5
Mud Plug	0.2	Spherical	0	200	200	3
Interbedded Sand	0.152	Spherical	0	860	860	8.7

Table 17: PHIE Variogram Models, Lower McMurray, taken from the Corner C pool.

5.1.3. Results and Discussion

A Sequential Gaussian Simulation (SGS) technique was used for PHIE simulation. A simple Kriging type was applied for PHIE simulation. PHIE was simulated simultaneously for all facies in the model, but was simulated separately for the two sub-sequences of the McMurray. For each facies, the PHIE upper and lower value limits were set to be 10% beyond the log data maximum and minimum for PHIE.

Five realizations for PHIE were simulated. In order to rank realizations for PHIE, pore volumes were calculated in 5 reservoir facies (Marine Sand, Interbedded Mud, Sand, and Interbedded Sand) (Table 18). Pore volumes were calculated by taking products between bulk cell volumes and corresponding PHIE values. The total reservoir pore volume for each realization is the sum of the pore volumes of all the cells. From Table 18, realization 2 for PHIE was chosen as a final PHIE distribution.

Realization	Pore Volumes (million m ³)
R1	38.274
R2	38.409
R3	38.802
R4	38.237
R5	38.624

Table 18: Pore Volumes for five different realizations – reservoir facies only (Marine Sand, Interbedded Mud, Sand, and Interbedded Sand)

A 3D view of the PHIE distribution is shown in Figure 27. A 2D view of the cross-section going through the available wells within the pool boundary is shown in Figure 28.

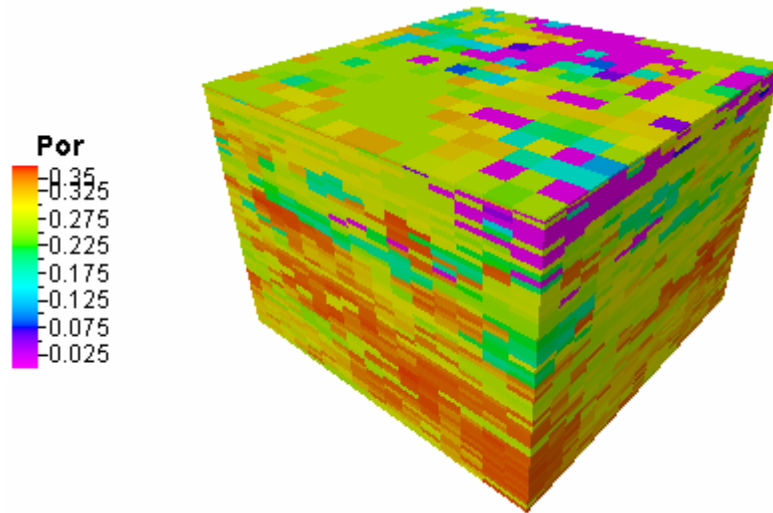


Figure 27: 3D View of the PHIE Distribution – Realization 2

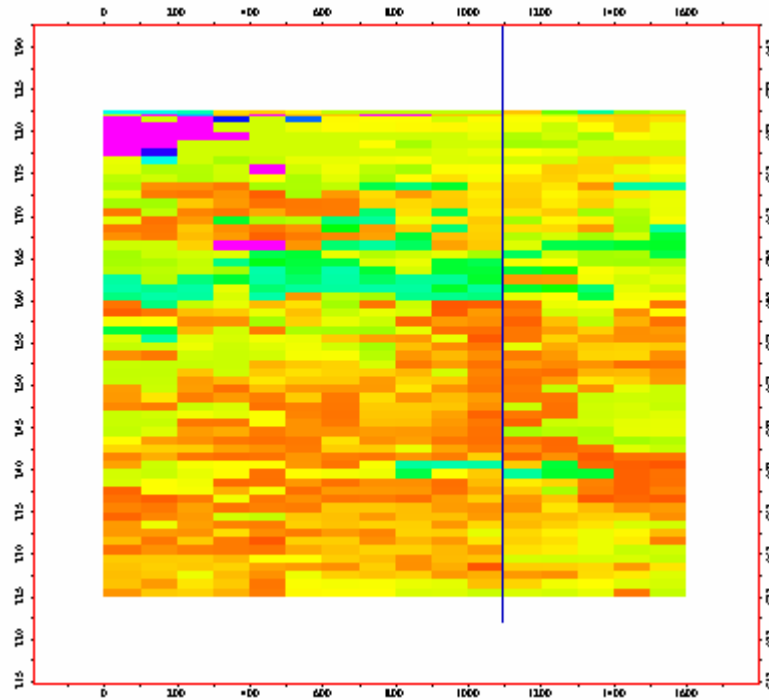


Figure 28: 2D View of the Cross Section Through Available Wells Showing PHIE Distribution

Histograms of the porosity distributions for each facies for both simulated and original log values are plotted in Figure 15 to Figure 26. The purpose of plotting PHIE histograms is to assess the quality of the simulation results. The shape of the histogram from simulated and log values are close. Table 19 and Table 20 list basic statistics for the PHIE simulated values. The basic

statistics of the simulated PHIE are very similar to the one from the original log data. This means that the simulation honors the input statistics.

Facies	PHIE simulation		
	Min	Max	Mean
Marine Mud	0.001	0.264	0.173
Marine Sand	0.280	0.322	0.310
Interbedded Mud	0.088	0.313	0.239
Interbedded Sand	0.001	0.328	0.183

Table 19: Statistics for simulated PHIE, A1 Sequence

Facies	PHIE simulation		
	Min	Max	Mean
Marine Mud	0.001	0.273	0.170
Marine Sand	0.268	0.344	0.303
Interbedded Mud	0.252	0.287	0.271
Sand	0.276	0.371	0.336
Mud Plug	0.189	0.224	0.209
Interbedded Sand	0.266	0.302	0.284

Table 20: Statistics for simulated PHIE, McMurray

5.2. Shale Volume (V_{sh})

5.2.1. Statistical Analysis

Facies	V_{sh} Original Logs			V_{sh} upscaled Logs		
	Min	Max	Mean	Min	Max	Mean
Marine Mud	0.230	0.390	0.160	0.272	0.272	0.272
Marine Sand	--	--	--	--	--	--
Interbedded Mud	--	--	--	--	--	--
Interbedded Sand	0.020	0.130	0.070	0.051	0.051	0.051

Table 21: Basic Statistics of V_{sh} for Different Facies-Original and Upscaled Logs, A1 Sequence

Facies	V_{sh} Original Logs			V_{sh} upscaled Logs		
	Min	Max	Mean	Min	Max	Mean
Marine Mud	0.300	0.360	0.060	0.334	0.334	0.334
Marine Sand	--	--	--	--	--	--
Interbedded Mud	0.110	0.490	0.380	0.220	0.288	0.069
Sand	0.000	0.390	0.078	0.000	0.257	0.077
Mud Plug	0.360	0.580	0.471	0.370	0.535	0.470
Interbedded Sand	0.000	0.530	0.080	0.004	0.260	0.073

Table 22: Basic Statistics of V_{sh} for Different Facies-Original and Upscaled Logs, Lower McMurray

Since several of the facies simulated do not have sufficient data, additional input statistics had to be specified to simulate V_{sh} . These values of minimum, maximum, mean, and standard deviation were taken from upscaled V_{sh} values from the appropriate facies in the Corner McMurray C model.

Facies	Min	Max	Mean	Standard Deviation
Marine Sand	0.000	0.0452	0.0194	0.0192
Interbedded Mud	0.000	0.7186	0.2809	0.2307

Table 23: Input statistics for V_{sh} taken from the Corner McMurray C pool, A1

Facies	Min	Max	Mean	Standard Deviation
Marine Sand	0.000	0.0286	0.0017	0.0057

Table 24: Input statistics for V_{sh} taken from the Corner McMurray C pool, Lower McMurray

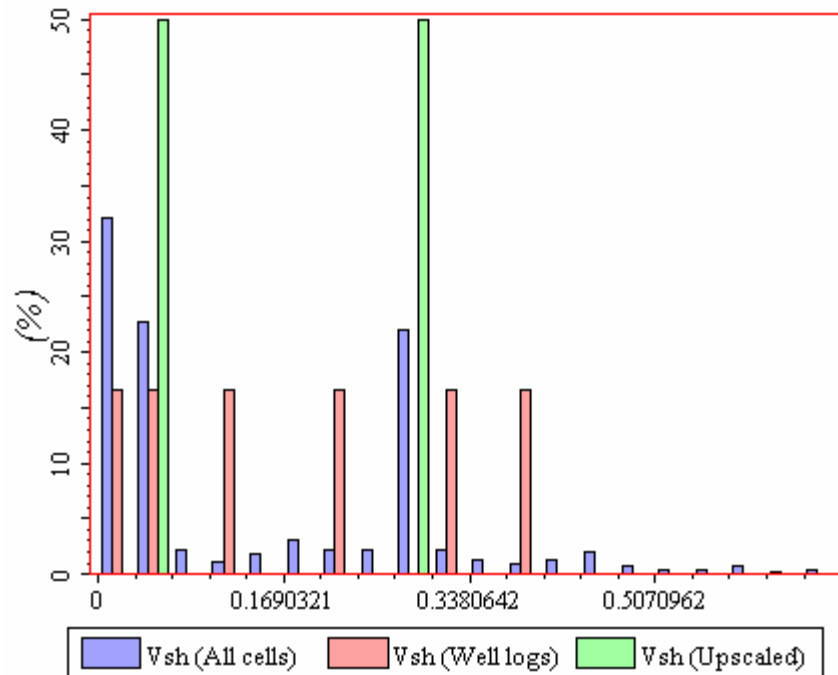


Figure 29: Upscaled and distributed values for V_{sh} - A1 all facies

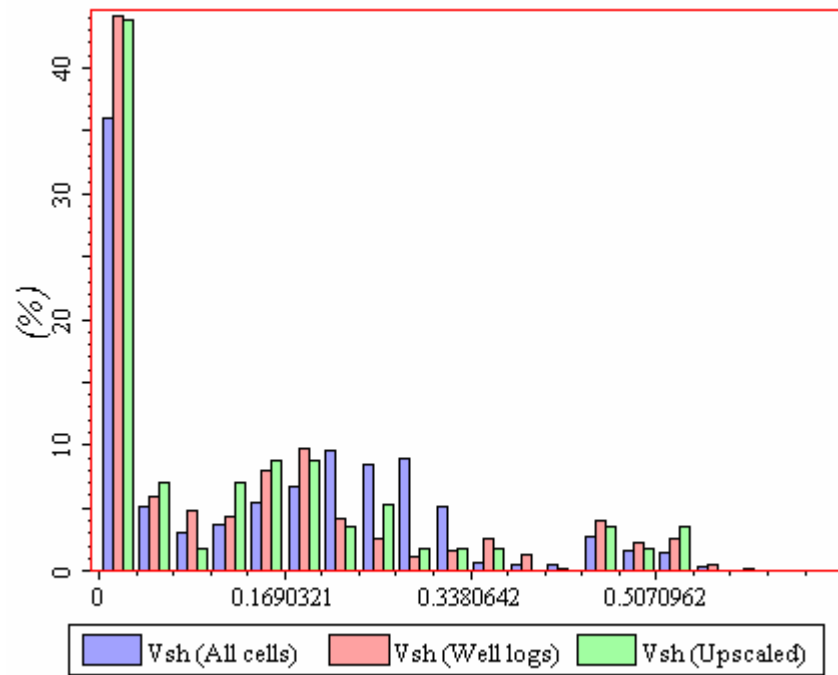


Figure 30: Upscaled and distributed values for VSh – Lower McMurray all facies

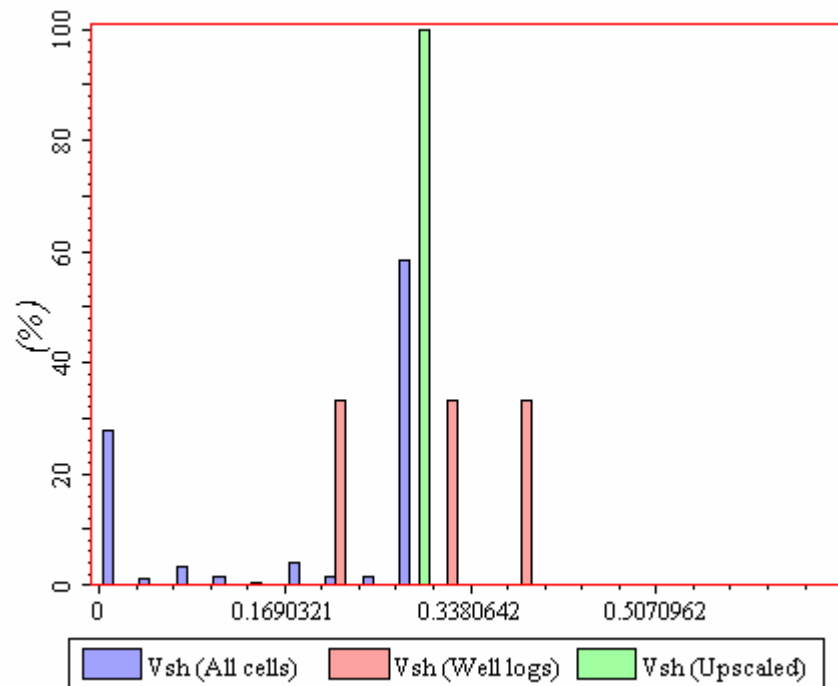


Figure 31: A1 Marine Mud V_{sh}

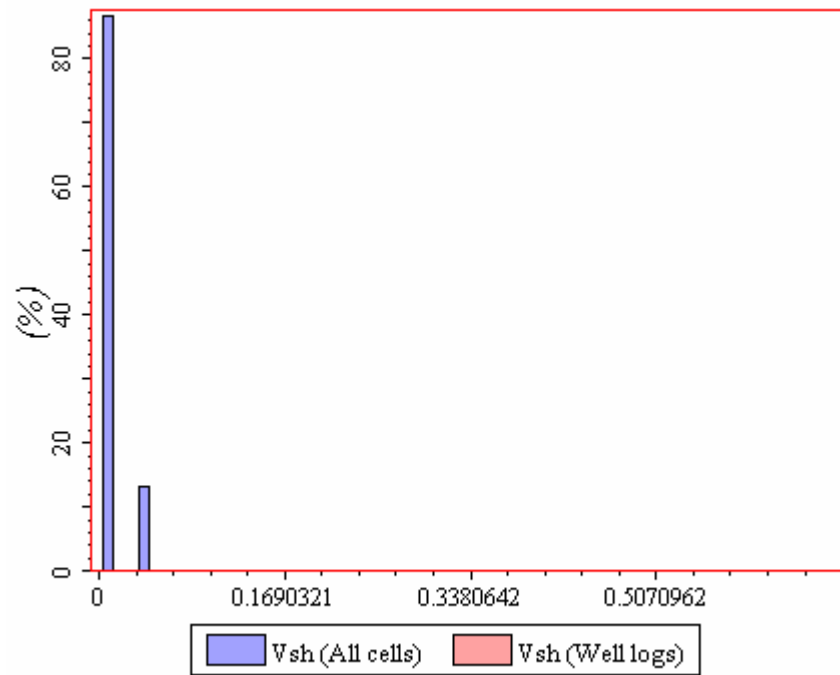


Figure 32: A1 Marine Sand V_{sh}

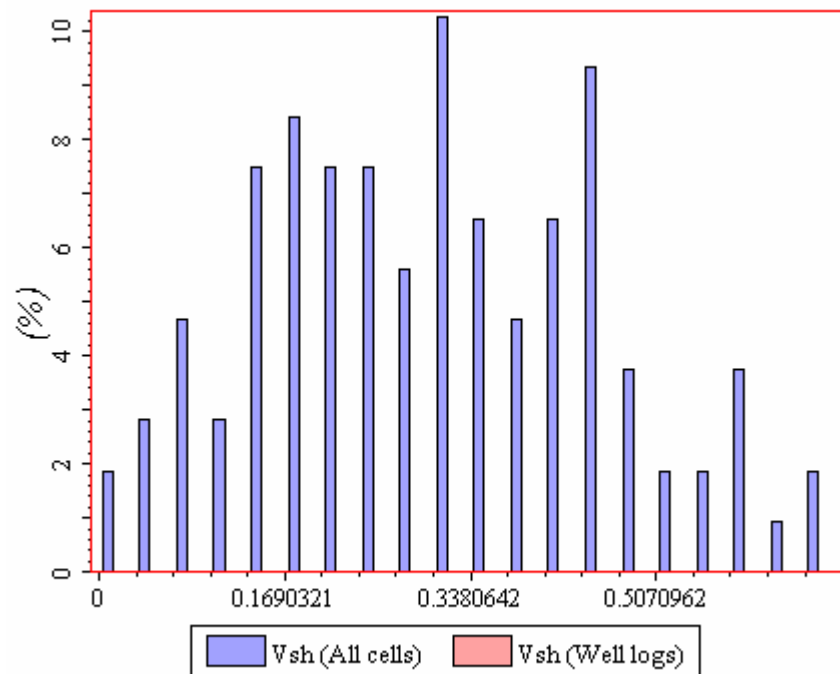


Figure 33: A1 Interbedded Mud V_{sh}

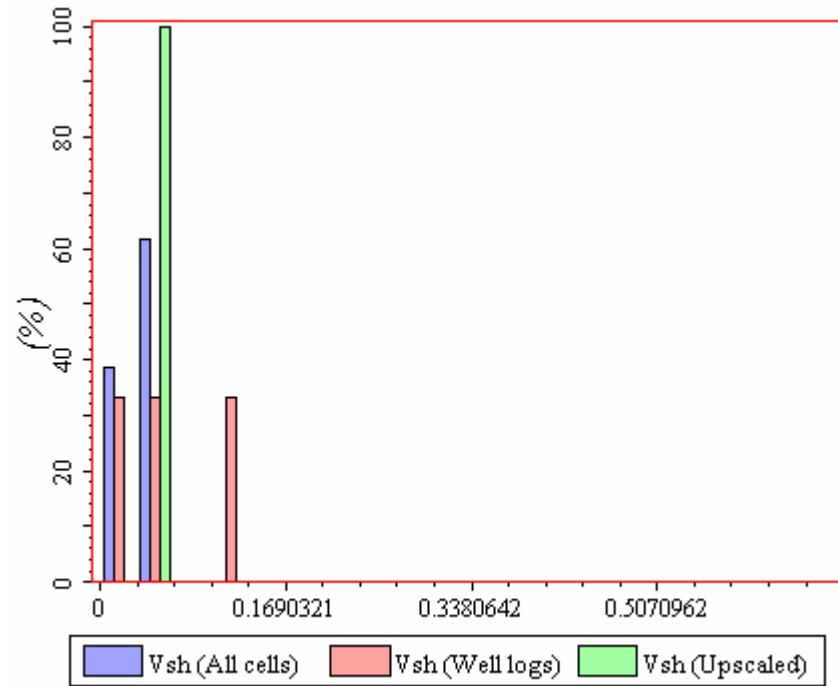


Figure 34: A1 Interbedded Sand V_{sh}

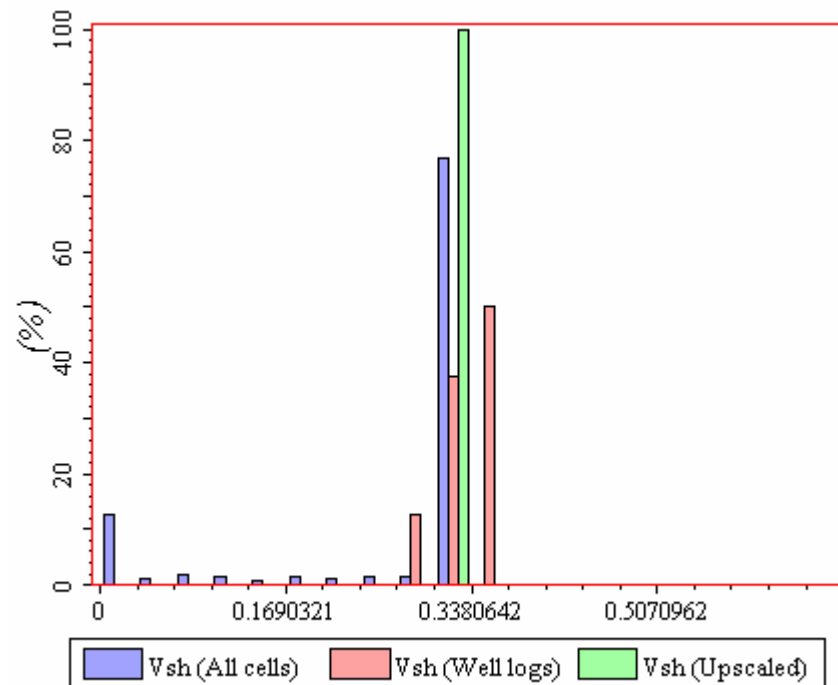


Figure 35: Lower McMurray Marine Mud V_{sh}

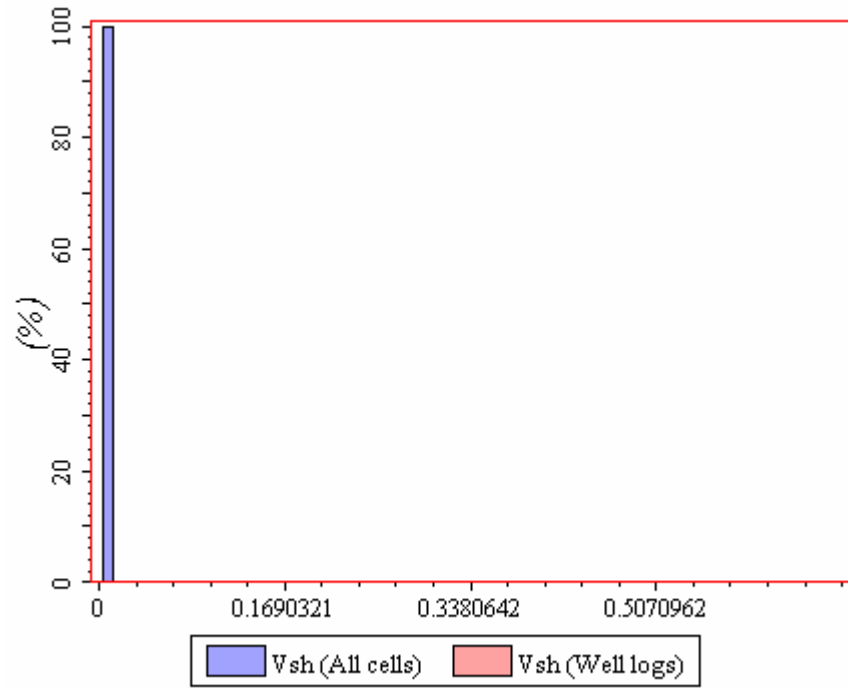


Figure 36: Lower McMurray Marine Sand V_{sh}

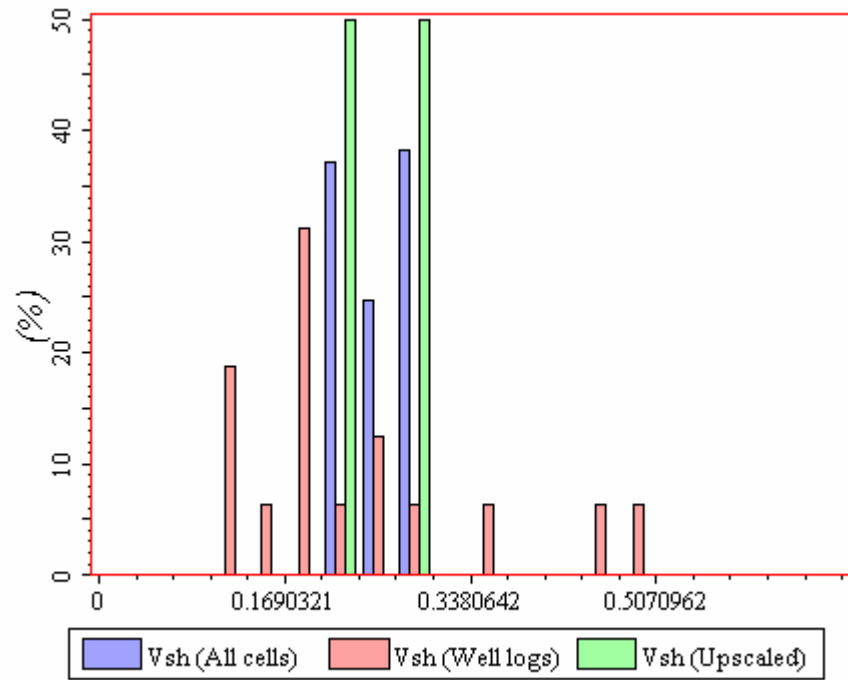


Figure 37: Lower McMurray Interbedded Mud V_{sh}

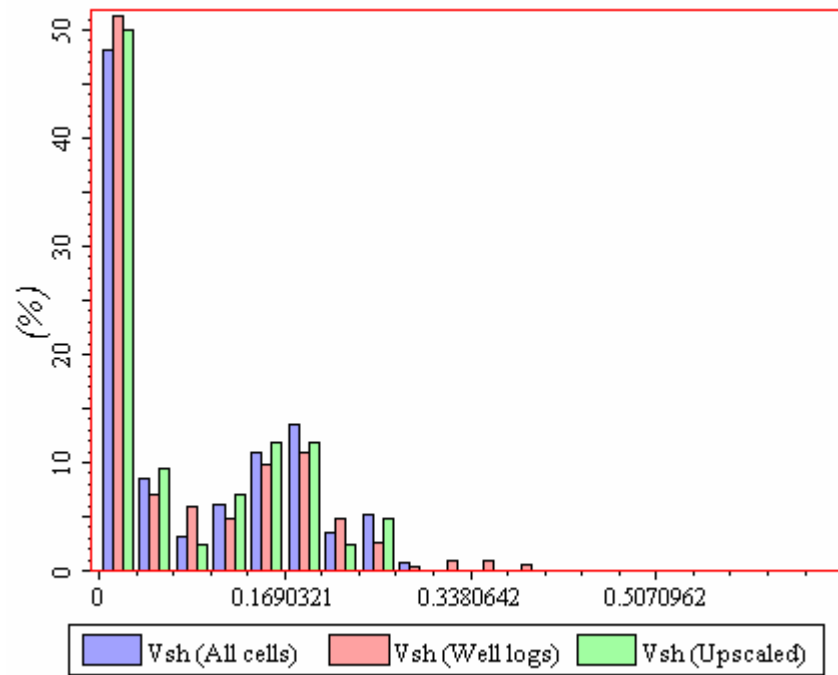


Figure 38: Lower McMurray Sand V_{sh}

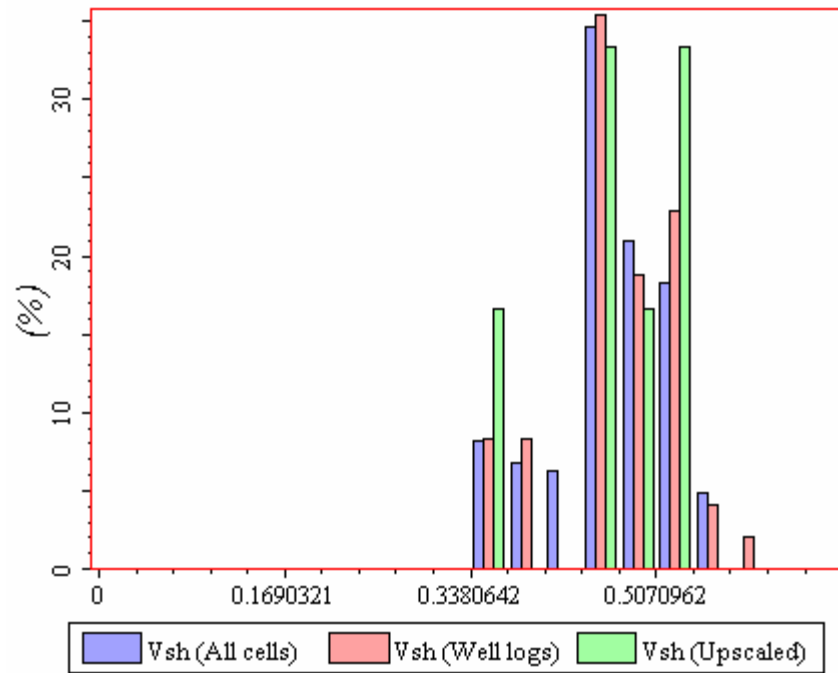


Figure 39: Lower McMurray Mud Plug V_{sh}

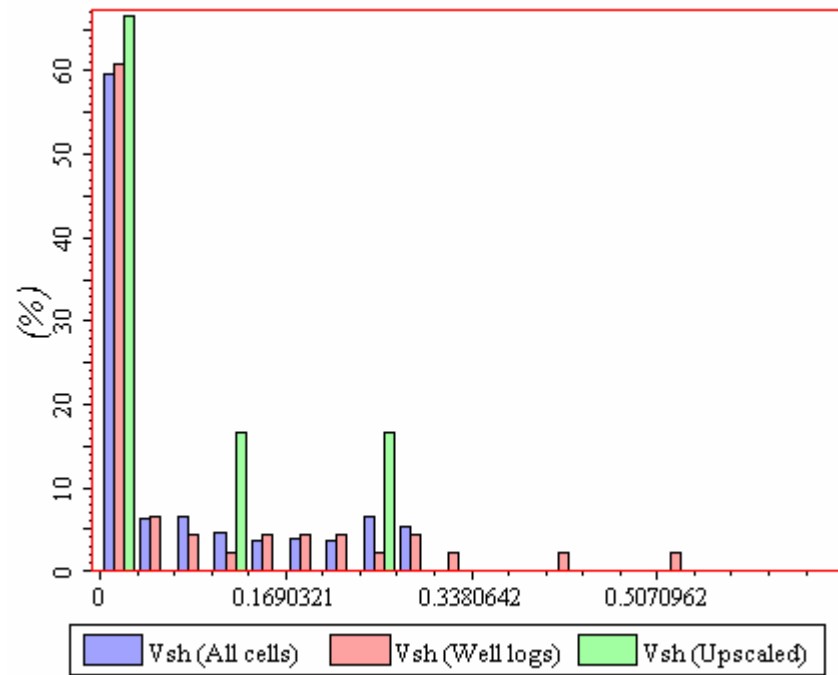


Figure 40: Lower McMurray Interbedded Sand V_{sh}

A crossplot of V_{sh} versus PHIE shows good correlation between the two parameters (Figure 41). Therefore, this correlation between V_{sh} and PHIE will be used in V_{sh} simulation.

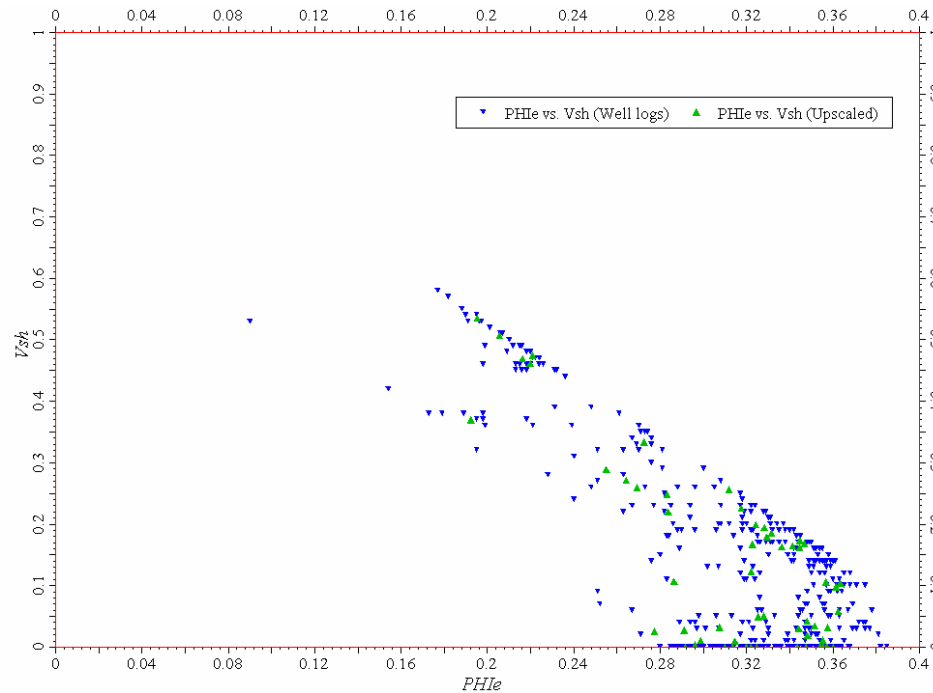


Figure 41: Crossplot between V_{sh} and PHIE

5.2.2. Variogram Analysis

Variogram models for V_{sh} for this single well pool were taken directly from the Corner C model (Table 25 and Table 26). More on V_{sh} variograms can be found in the similar report for the Corner C pool.

Facies	Nugget	Type	Anisotropy Angle	Ranges (m)		
				Major	Minor	Vertical
Marine Mud	0.2	Spherical	0	1000	1000	5.6
Marine Sand	0.2	Exponential	0	1000	1000	4.1
Interbedded Mud	0.237	Exponential	0	500	500	20
Interbedded Sand	0.085	Spherical	0	500	500	8

Table 25: V_{sh} Variogram Models – A1, taken from the Corner C pool

Facies	Nugget	Type	Anisotropy Angle	Ranges (m)		
				Major	Minor	Vertical
Marine Mud	0.2	Spherical	0	1000	1000	5.6
Marine Sand	0.261	Spherical	0	1000	1000	4.1
Interbedded Mud	0.2	Exponential	0	500	500	20
Sand	0.2	Spherical	0	1000	500	6
Breccia	0.2	Spherical	0	50	50	4.7
Mud Plug	0.2	Spherical	0	200	200	3
Interbedded Sand	0.2	Spherical	0	500	500	8

Table 26: V_{sh} Variogram Models – McMurray, taken from the Corner C pool

5.2.3. Results and Discussion

Sequential Gaussian Simulation was used for V_{sh} simulation. V_{sh} was also cokriged with PHIE. Correlation coefficients between V_{sh} and PHIE from Table 27 were used for each facies. For A1, these correlation coefficients were taken from the Corner C model. The coefficients for the McMurray were determined in a function window in Petrel using the unfiltered data points from the upscaled well logs.

Cokriging was not used for the two facies with only one data point.

Facies	Correlation Coefficients between V_{sh} and PHIE	
	A1	Lower McMurray
Marine Mud	-0.745	One data point
Marine Sand	-0.767	One data point
Interbedded Mud	-0.844	-0.5
Sand	--	-0.283
Mud Plug	--	0.144

Interbedded Sand	-0.459	-0.659
------------------	--------	--------

Table 27: Correlation between V_{sh} and PHIE by Facies

Five realizations of V_{sh} were generated. In order to rank those realizations, the average shale volumes of interbedded sand and interbedded mud were calculated and ranked for each realization (Table 28). Shale volumes were calculated by taking products between the cell volumes and corresponding V_{sh} values. Realization 1 was the midpoint of the ranking, therefore it was chosen for further consideration.

Realization	Average V_{sh} in Interbedded mud and Interbedded sand facies
R1	0.1568
R2	0.1550
R3	0.1592
R4	0.1588
R5	0.1542

Table 28: Shale Volumes for Five Different Realizations

Comparison between simulated V_{sh} values and original log data is shown in Figure 29 to Figure 40. A crossplot of simulated V_{sh} versus PHIE is shown in Figure 42. The crossplot shows that simulated V_{sh} values have similar correlation with PHIE compared with the original log values.

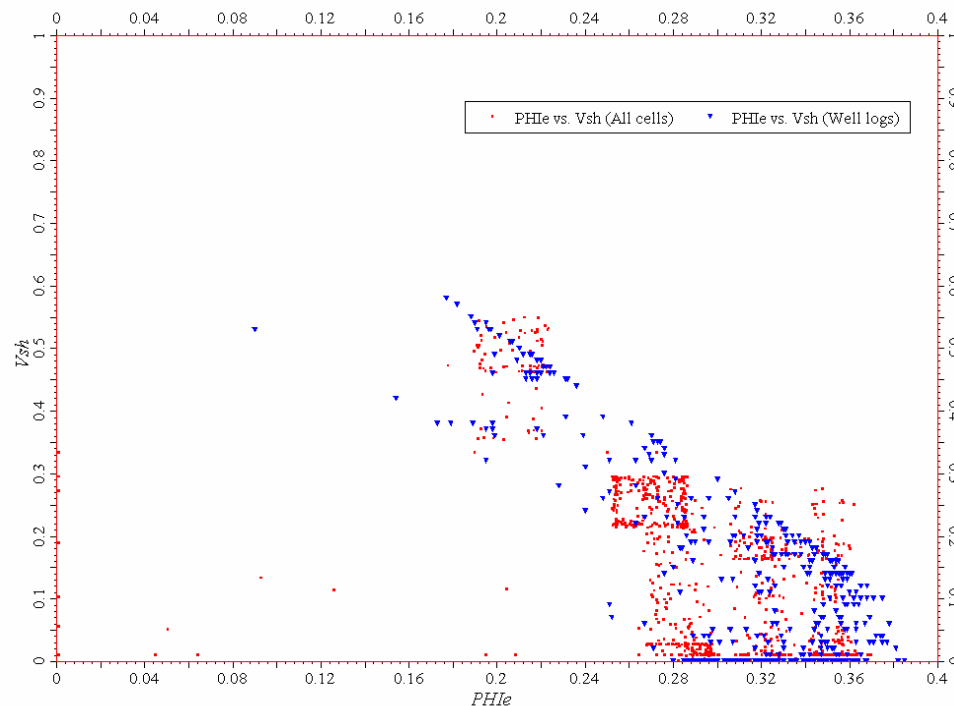


Figure 42: Cross Plot of V_{sh} and PHIE for Simulation and Original Well Logs

A 3D view of the V_{sh} distribution in the McMurray formation is depicted in Figure 43. Also, a cross-sectional view through 12-28 is captured in Figure 44.

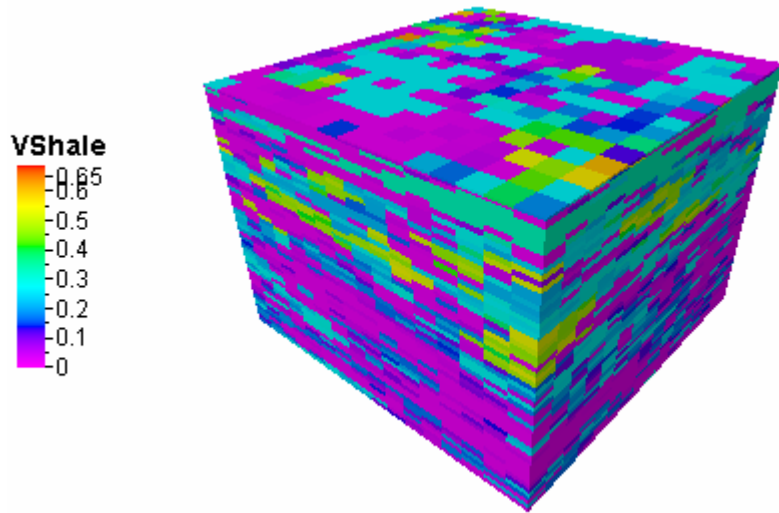


Figure 43: 3D View of the V_{sh} Distribution

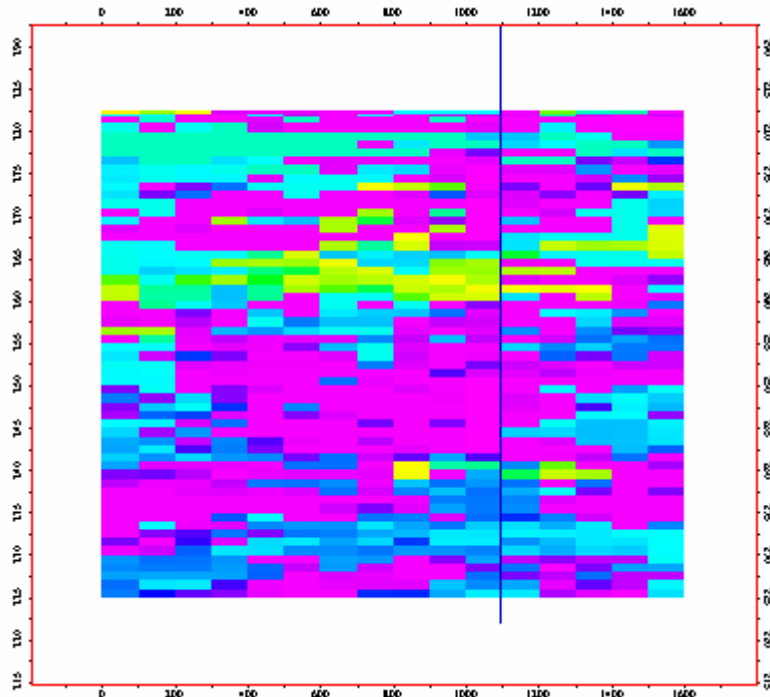


Figure 44: 2D View of the Cross Section Through Available Wells Showing V_{sh} Distribution

Basic statistics for V_{sh} simulated values are given below. The simulated V_{sh} values have similar distribution for all the facies compared with the original log data.

Facies	V_{sh} simulation		
	Min	Max	Mean
Marine Mud	0.010	0.272	0.183
Marine Sand	0.012	0.044	0.024
Interbedded Mud	0.019	0.676	0.313
Interbedded Sand	0.010	0.05	0.035

Table 29: Statistics for simulated VSh, A1 Sequence

Facies	V_{sh} simulation		
	Min	Max	Mean
Marine Mud	0.010	0.334	0.275
Marine Sand	0.000	0.016	0.003
Interbedded Mud	0.213	0.295	0.254
Sand	0.000	0.282	0.086
Mud Plug	0.353	0.551	0.468
Interbedded Sand	0.004	0.285	0.077

Table 30: Statistics for simulated VSh, Lower McMurray

5.3. Water Saturation (S_w)

5.3.1. Statistical Analysis

Water saturation values were available in log data. Therefore, S_w will be analyzed and simulated first, then the bitumen saturation and gas saturation will be calculated depending on the fluid present in the reservoir.

Facies	S_w Original Logs			S_w upscaled Logs		
	Min	Max	Mean	Min	Max	Mean
Marine Mud	0.840	0.900	0.870	0.856	0.856	0.856
Marine Sand	--	--	--	--	--	--
Interbedded Mud	--	--	--	--	--	--
Interbedded Sand	0.730	0.810	0.770	0.754	0.754	0.754

Table 31: Basic Statistics of S_w for Different Facies-Original and Upscaled Logs, A1 Sequence

Facies	S _w Original Logs			S _w upscaled Logs		
	Min	Max	Mean	Min	Max	Mean
Marine Mud	0.450	0.500	0.477	0.476	0.476	0.476
Marine Sand	--	--	--	--	--	--
Interbedded Mud	0.240	0.590	0.459	0.450	0.491	0.470
Sand	0.120	0.660	0.247	0.129	0.627	0.247
Mud Plug	0.490	0.790	0.704	0.546	0.760	0.703
Interbedded Sand	0.280	0.740	0.481	0.374	0.700	0.483

Table 32: Basic Statistics of S_w for Different Facies-Original and Upscaled Logs, Lower McMurray

Since several of the facies simulated do not have sufficient data, additional input statistics had to be specified to simulate S_w. These values of minimum, maximum, mean, and standard deviation were taken from upscaled S_w values from the appropriate facies in the Corner McMurray C model.

Facies	Min	Max	Mean	Standard Deviation
Marine Sand	0.369 1	0.688 8	0.552 8	0.0732
Interbedded Mud	0.438 0	0.835 2	0.537 1	0.0924

Table 33: Additional Statistics for S_w taken from Corner McMurray C pool, A1

Facies	Min	Max	Mean	Standard Deviation
Marine Sand	0.206	0.542	0.334	0.092

Table 34: Additional Statistics for S_w taken from Corner McMurray C pool, Lower McMurray

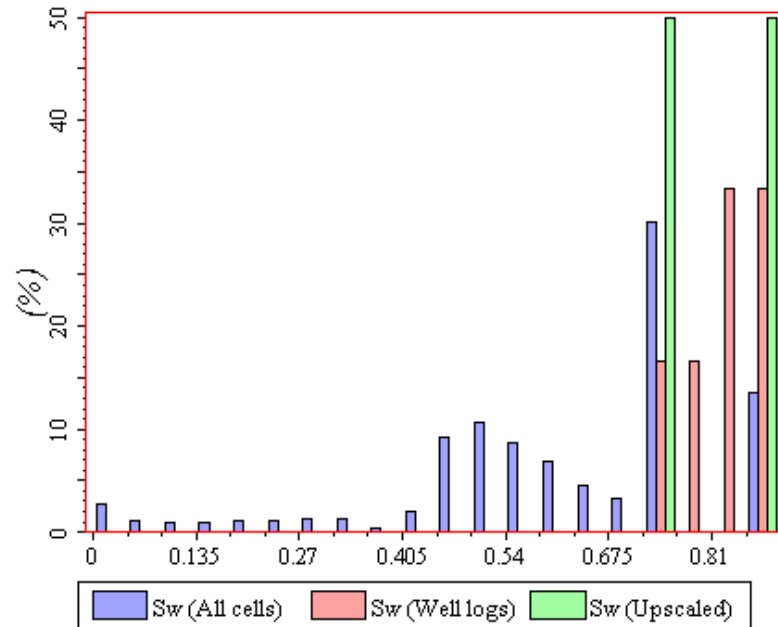


Figure 45: Upscaled and distributed values for S_w - A1 all facies

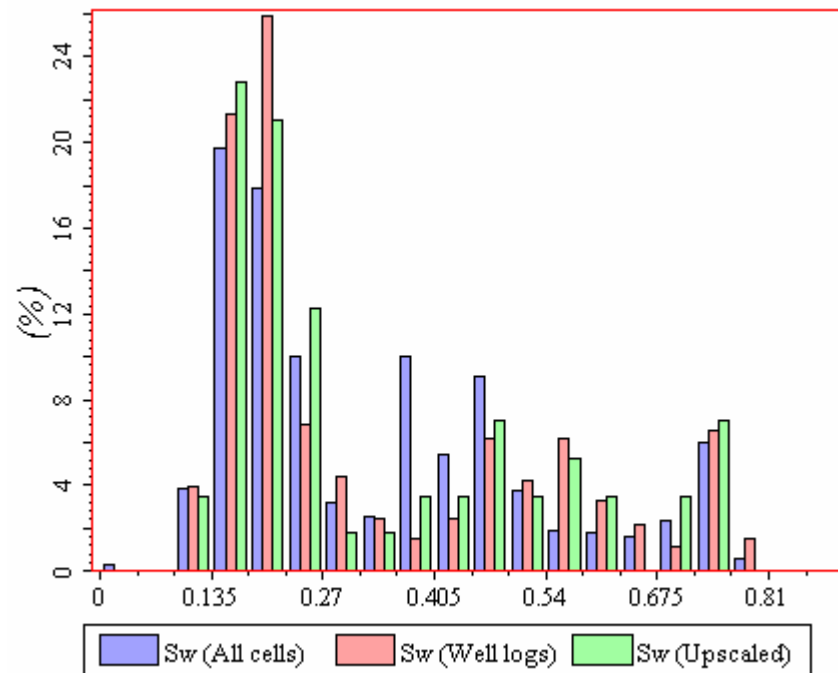


Figure 46: Upscaled and distributed values for S_w - Lower McMurray all facies

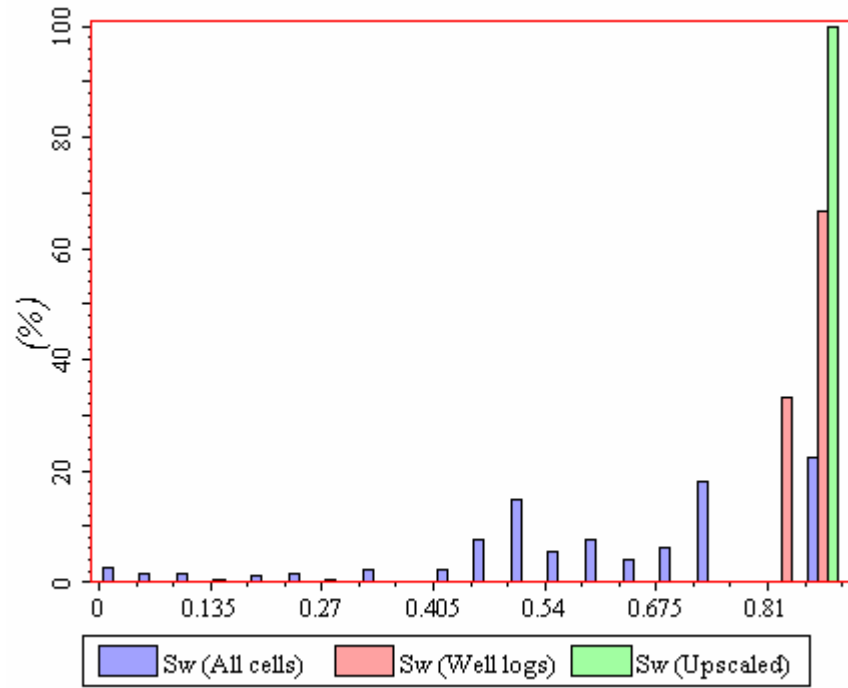


Figure 47: A1 Marine Mud S_w

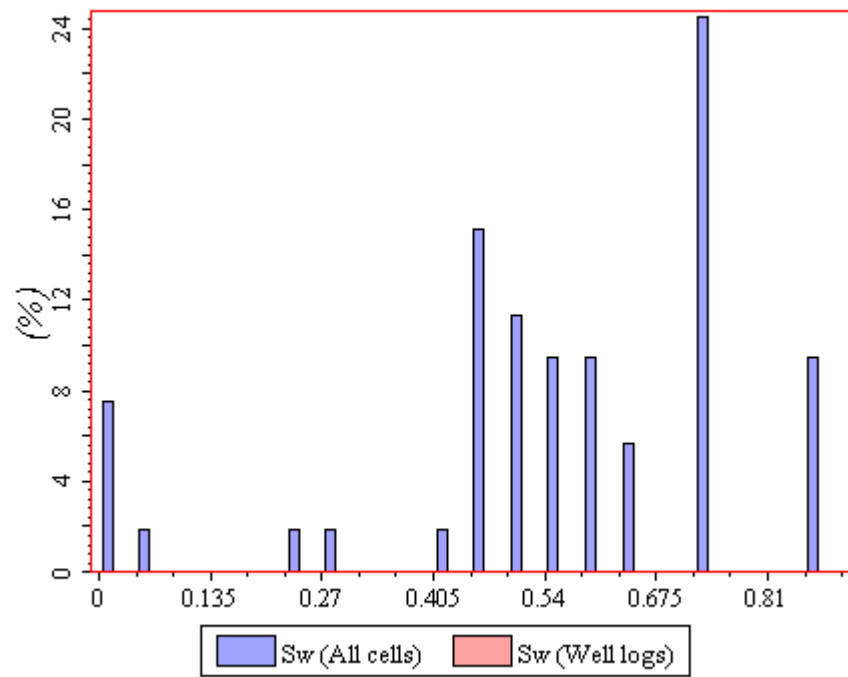


Figure 48: A1 Marine Sand S_w

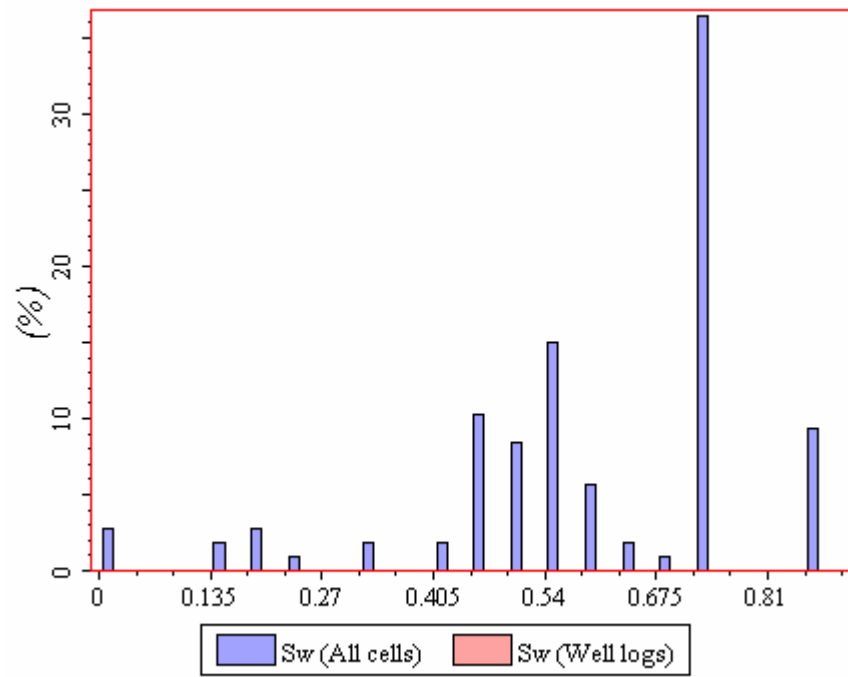


Figure 49: A1 Interbedded Mud S_w

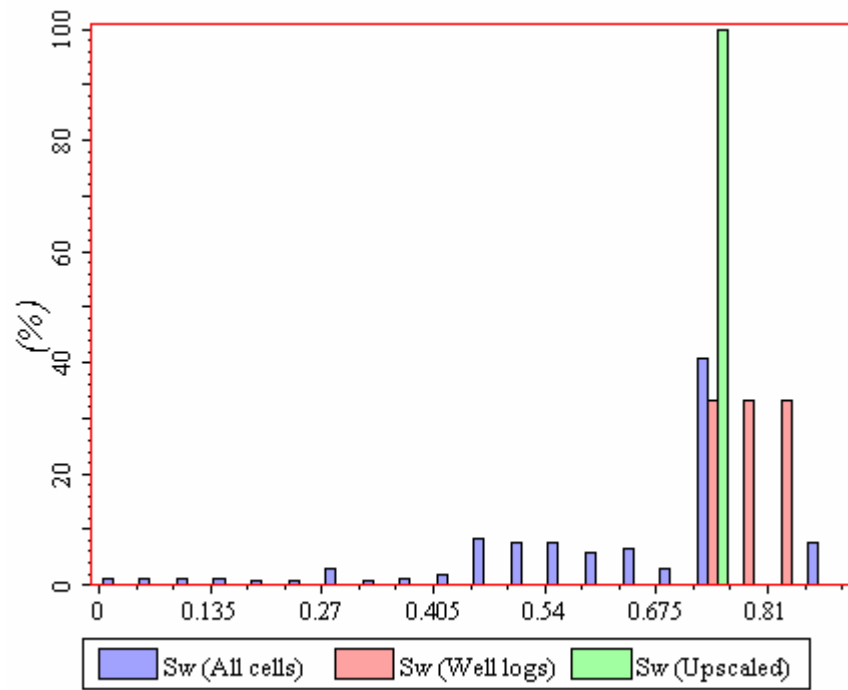


Figure 50: A1 Interbedded Sand S_w

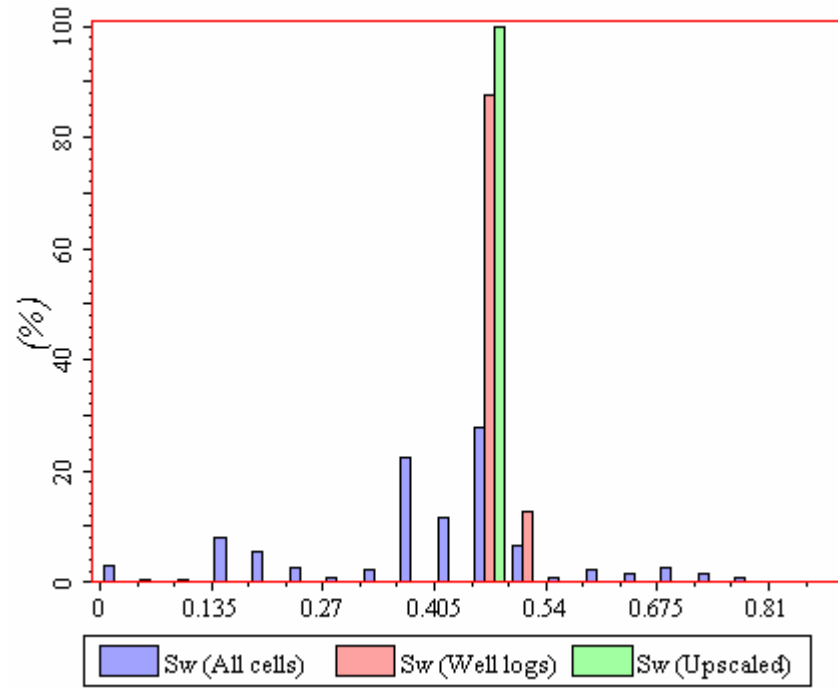


Figure 51: Lower McMurray Marine Mud S_w

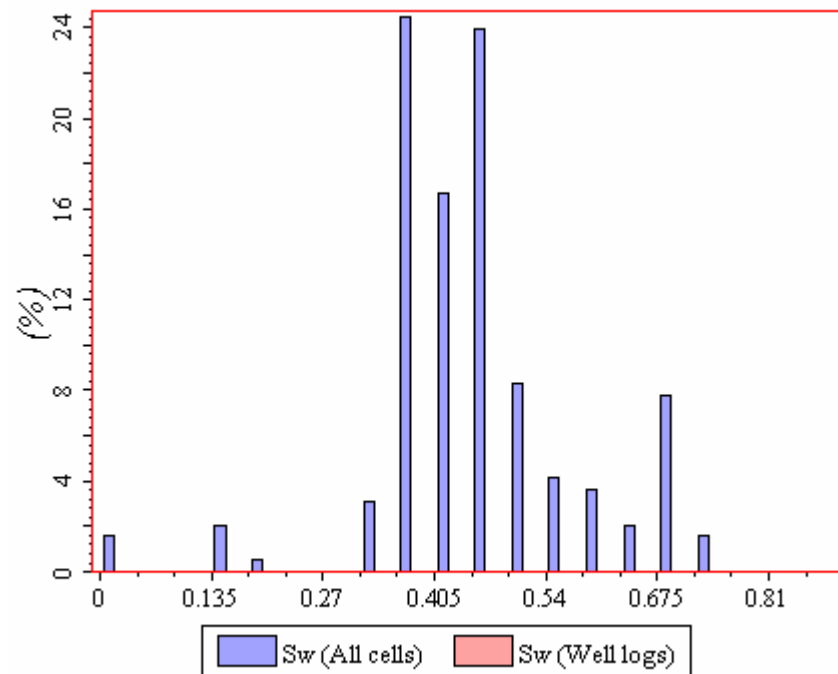
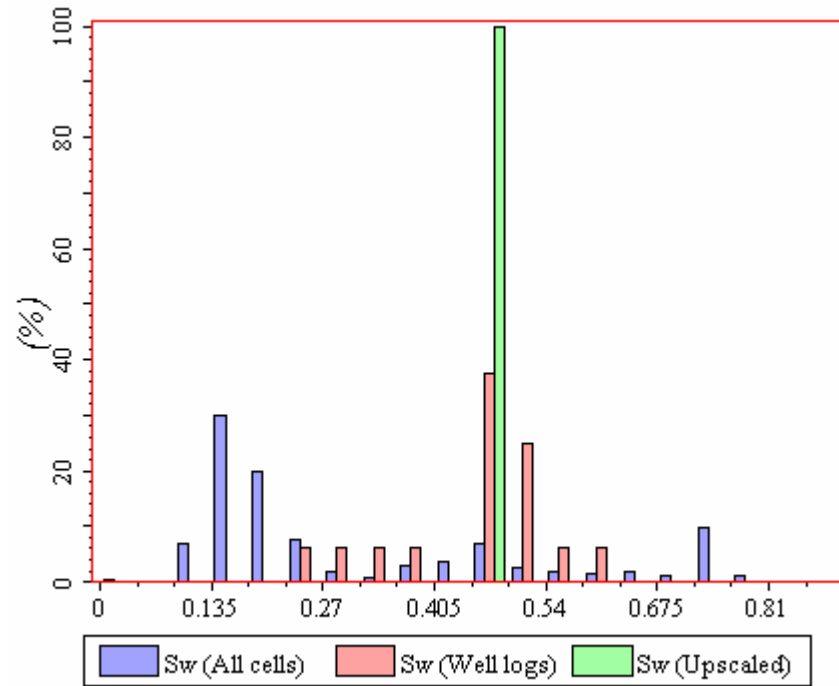
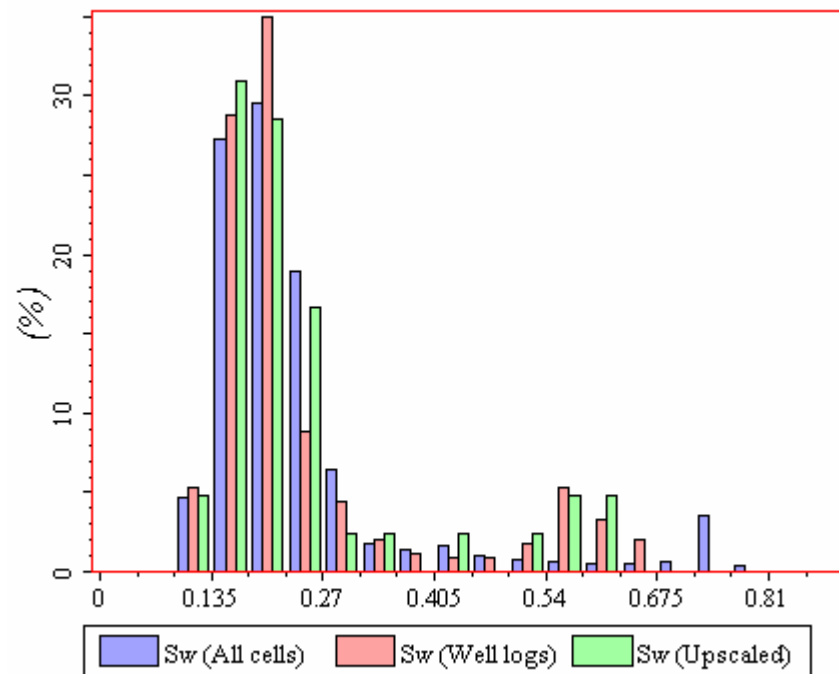


Figure 52: Lower McMurray Marine Sand S_w

Figure 53: Lower McMurray Interbedded Mud S_w Figure 54: Lower McMurray Sand S_w

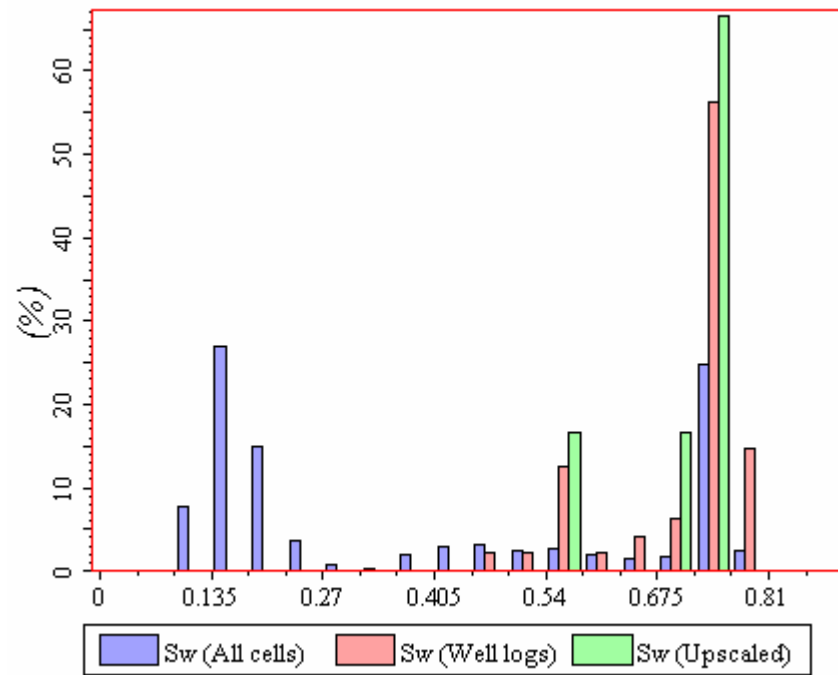


Figure 55: Lower McMurray Mud Plug S_w

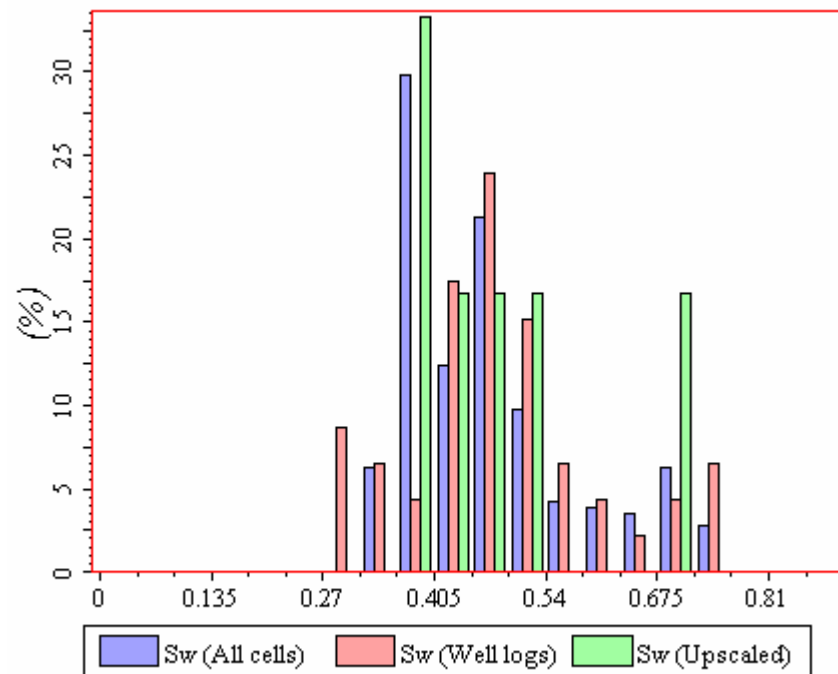


Figure 56: Lower McMurray Interbedded Sand S_w

5.3.2. Zonation

To correctly identify correlations between water saturation and porosity, the water zones in the well logs were identified and filtered out. To perform this filtering, fluids zone boundaries were identified in the 12-28 well location. Data points that are in the water zone were removed from the variogram analysis and simulation of the S_w property. These fluid zone boundaries were then propagated throughout the entire grid. These boundaries were also later used to calculate the S_o and S_g in the model, by differentiating between water, gas, and oil zones.

The effect of the water filter on the upscaled values is shown in the following crossplots. The cutoffs only affected certain facies, and only in the lower McMurray.

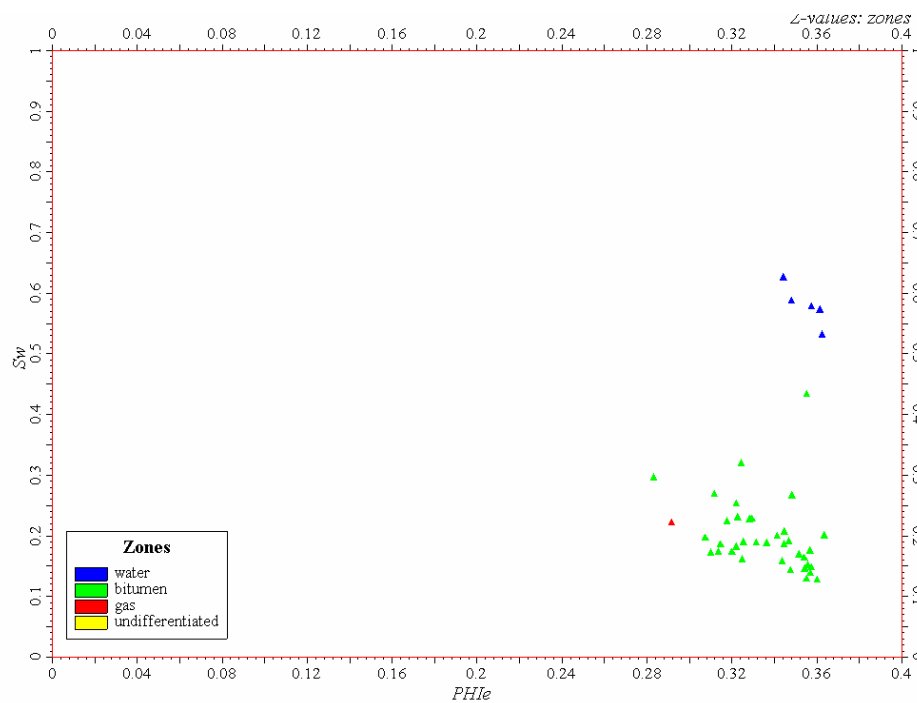


Figure 57: Water Zone cutoffs for Lower McMurray Sand facies

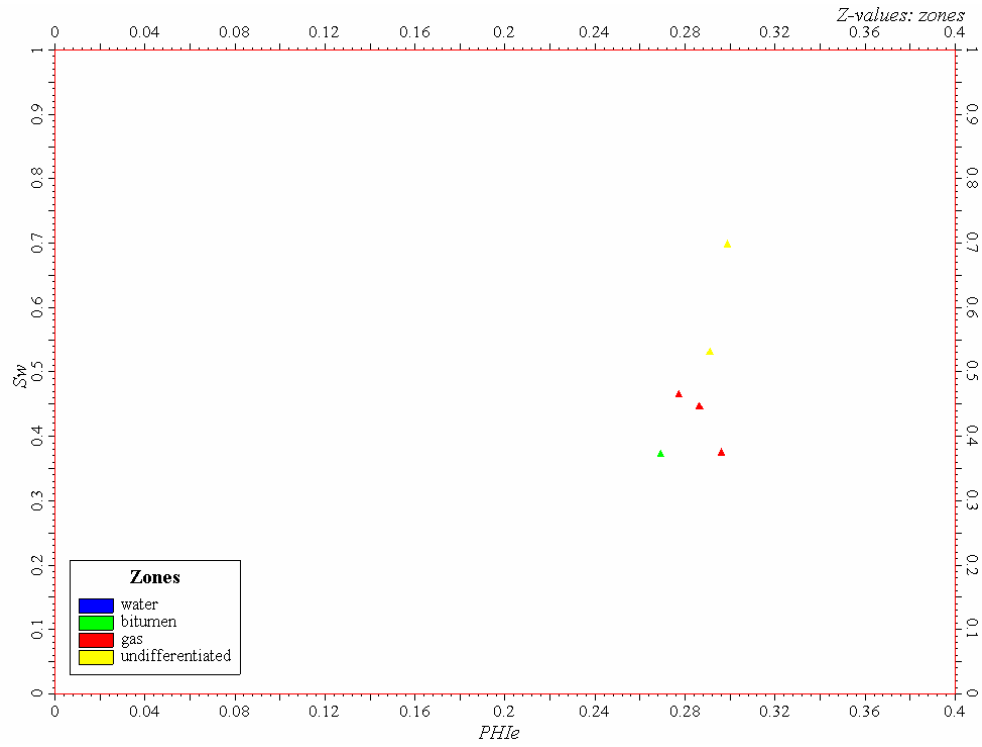


Figure 58: Water Zone cutoffs Lower McMurray Interbedded Sand

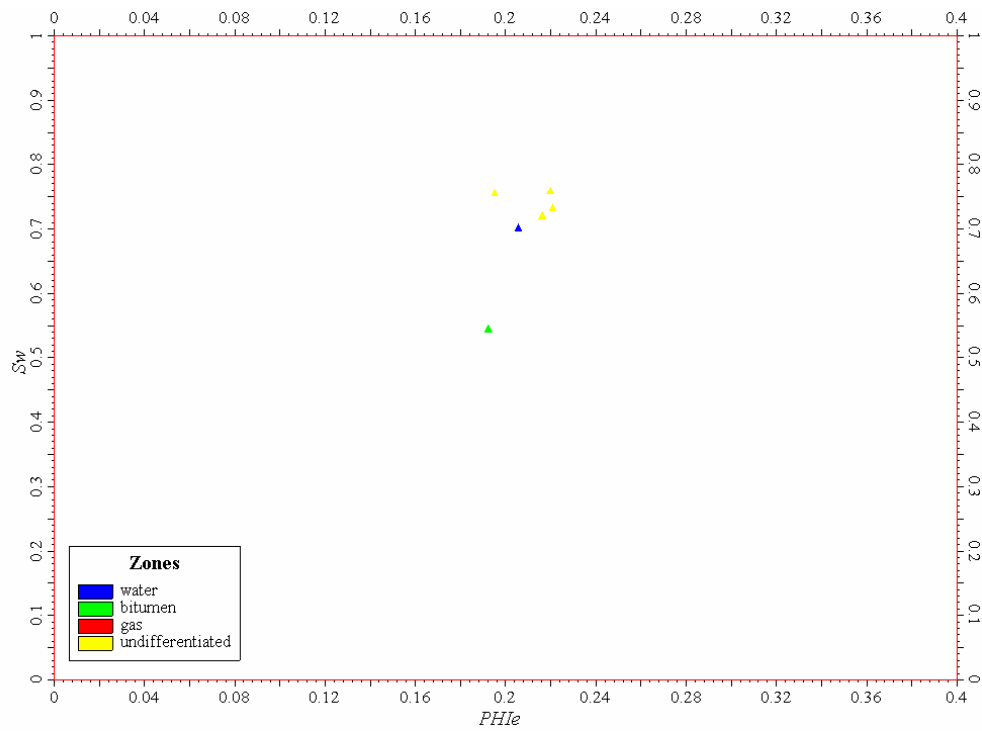


Figure 59: Water zone cutoffs for Lower McMurray Mud Plug

5.3.3. Variogram Analysis

Variograms for S_w were taken from the Corner McMurray C model. Table 35 and Table 36 list S_w variogram models for each of the facies.

Facies	Nugget	Type	Anisotropy Angle	Ranges (m)		
				Major	Minor	Vertical
Marine Mud	0.2	Spherical	0	1000	1000	6
Marine Sand	0.04	Spherical	0	1428.4	1234.9	1.5
Interbedded Mud	0.2	Spherical	0	1138.2	828.8	1.4
Interbedded Sand	0.2	Spherical	0	1400	1400	2

Table 35: S_w Variogram Models – A1, taken from the Corner C pool

Facies	Nugget	Type	Anisotropy Angle	Ranges (m)		
				Major	Minor	Vertical
Marine Mud	0.2	Spherical	0	1000	1000	6
Marine Sand	0.081	Spherical	0	2200	2200	1.4
Interbedded Mud	0.112	Spherical	0	500	500	8.2
Sand	0.072	Spherical	0	1000	1000	9.9
Breccia	0.2	Spherical	0	50	50	2
Mud Plug	0.2	Spherical	0	200	200	5
Interbedded Sand	0.2	Spherical	0	1000	1000	11.1

Table 36: S_w Variogram Models – Lower McMurray, taken from the Corner C pool

5.3.4. Results and Discussion

Sequential Gaussian Simulation (SGS) was used for S_w simulation. A co-kriging option was used with PHIE as a co-kriged property. The correlation coefficients were taken from Corner C for the A1 zone and were calculated from a function window in Petrel for the Lower McMurray zone. They are listed in Table 37. Again, these correlations were obtained with the water zone filtered out, so they are applicable only to the bitumen / gas zones. With the water zone filtered out, only one data point remained for the Marine Mud facies in both zones. This facies was not simulated with the co-kriging option.

Facies	Correlation Coefficients between V_{sh} and PHIE	
	A1	McMurray
Marine Mud	One data point – not cokriged	One data point – not cokriged
Marine Sand	-0.633	One data point – not cokriged
Interbedded Mud	-0.688	0.5
Sand	--	-0.290
Mud Plug	--	0.482

Interbedded Sand	-0.715	0.417
------------------	--------	-------

Table 37: Correlation between S_w and PHIE by Facies

Again, five (5) realizations were generated for S_w , one of which will be considered in the final result. These realizations were generated with the water zones filtered out.

In order to rank 5 realizations for S_w , the average water saturation over 5 reservoir facies was calculated (Marine Sand, Interbedded Mud, Breccia, Sand, and Interbedded Sand). The results are presented in Table 38. Realization 5 was chosen.

Realization	Average S_w
R1	0.3384
R2	0.3325
R3	0.3286
R4	0.3309
R5	0.3310

Table 38: Average S_w over 5 reservoir facies, by realization

Figure 60 shows a 3D view of the S_w values for realization 5. Figure 61 shows the cross-section of S_w through 12-28.

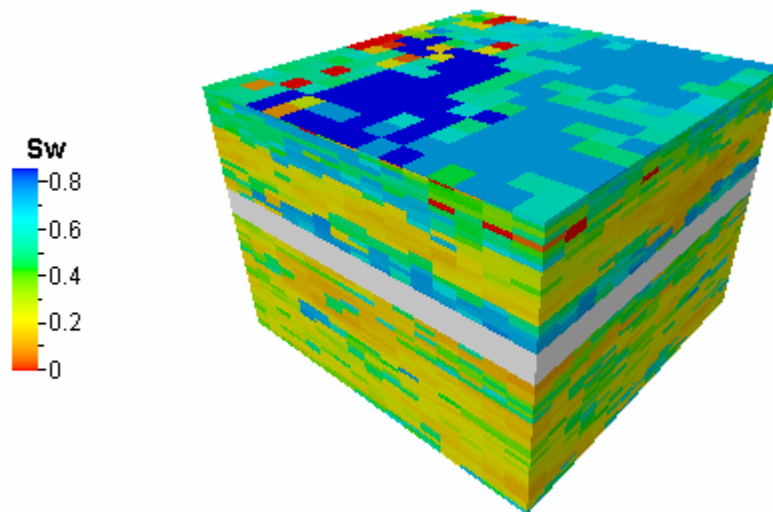


Figure 60: 3D View of the S_w Distribution – Realization 5. Grey areas are filtered out with the water zone filter.

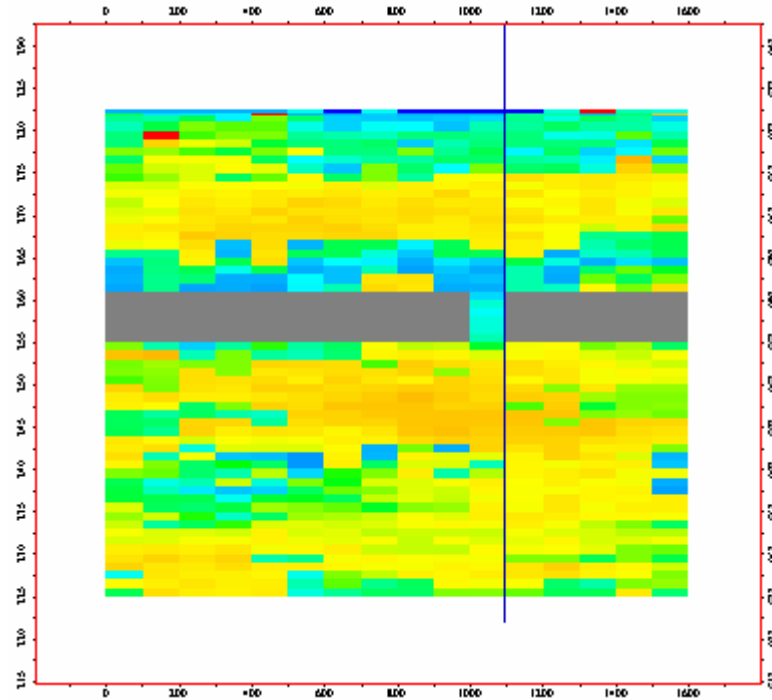


Figure 61: 2D View of the Cross-Section Through Available Wells Showing S_w Distribution. Grey areas are filtered out with the water zone filter.

After the S_w distribution was populated, the next step was to determine the final S_w , S_g and S_o values. The boundaries of the gas, top water and bottom water pools were drawn out to the section boundary from the well data. Figure 62 illustrates these fluid boundaries in a 3D view.

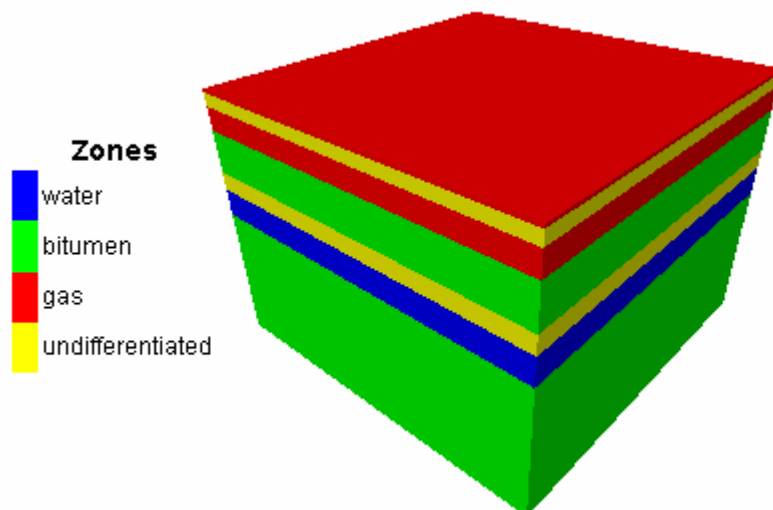


Figure 62: Gas, Bitumen and Water Zones for the Section 12-28 Pool

In the water zone, S_w is set to 1.

In the gas zone, the S_g values were calculated using the equation $S_g = 1 - S_w$. In the water and bitumen zones, S_g values are zero (0).

In the bitumen zone, the S_o values were calculated using the equation $S_o = 1 - S_w$. In the gas or water zones, the S_o values are zero (0).

Below are figures showing snapshots of S_w , S_g and S_o distributions for the Section 12-28 pool.

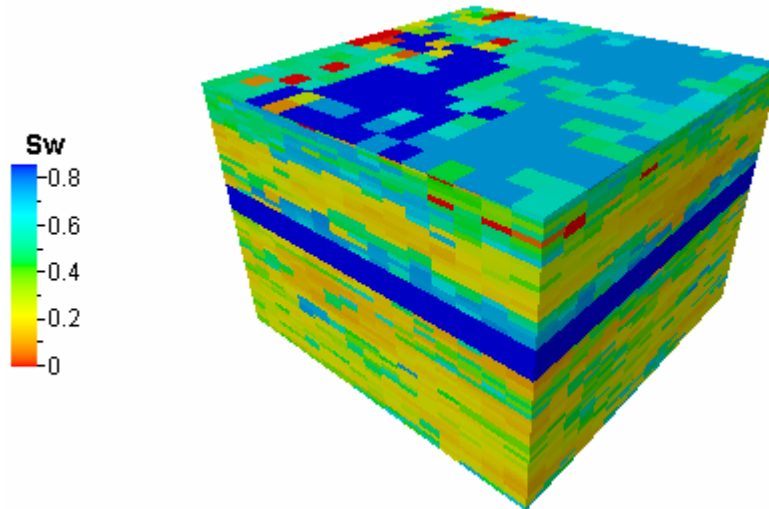


Figure 63: S_w Distribution for the 12-28 pool

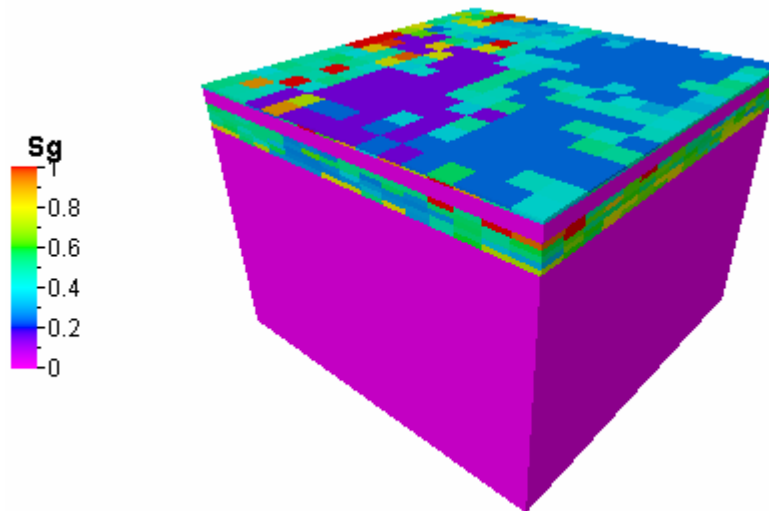


Figure 64: S_g Distribution for the 12-28 pool

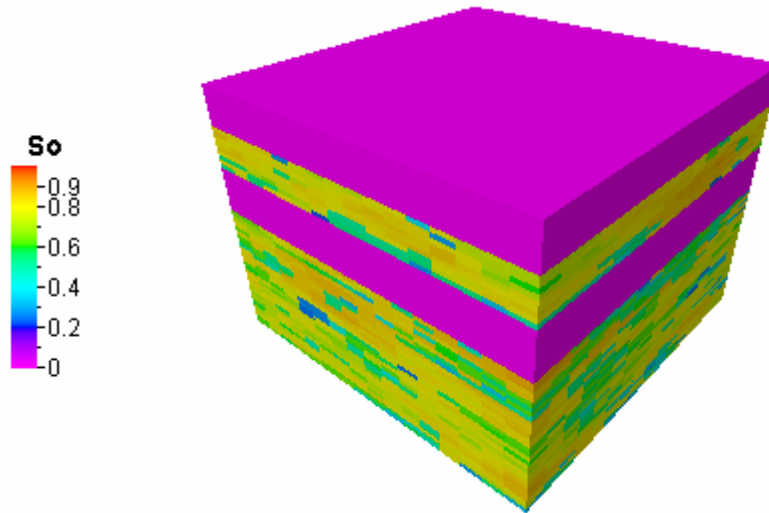


Figure 65: S_o Distribution for the 12-28 pool

A1 Sequence	Total PV	Water PV	Gas PV	Bit PV	Undifferentiated PV
A1 gas			0.381315		
Total A1	0.381315	0	0.381315	0	0

Table 39: Pore volumes in A1 Sequence by fluid zone. Porosity ≥ 0.16 , Shale Volume ≤ 0.60 , in millions m^3

McMurray	Total PV	Water PV	Gas PV	Bit PV	Undifferentiated PV
Top water		4.905921			
Top bitumen		7.525163			
Lower bitumen			25.26988		
Top gas				3.78735	4.323388
Total McMurray	45.8117	12.43108	25.26988	3.78735	4.323388

Table 40: Pore volumes in Lower McMurray by fluid zone. Porosity ≥ 0.16 , Shale Volume ≤ 0.60 , in millions m^3

5.4. Horizontal Permeability

Horizontal permeability was calculated based on the correlation provided in the petrophysical analysis report for the Section 12-28 pool [4]. This correlation was derived from a cross-plot between PHIE and core permeability.

$$k_h = 10^{(18.3 \cdot \text{PHIE} - 3)} \quad (1)$$

The values of k_h were calculated globally for all the facies based on the final realization 2 for PHIE as described in the previous section for PHIE

simulation. Figure 66 shows a 3D view of the calculated k_h for the Section 12-28 pool. Figure 67 shows a histogram of calculated horizontal permeability.

It should be mentioned that extreme values (very high or very low) from the calculated k_h were reassessed. This k_h reassignment was necessary because formula (1) does not specify the limit for PHIE, within which the formula is valid. The formula was derived from a regression of the core dataset that did not cover the whole range of the PHIE data for the Section 12-28 pool. Extreme values, especially the lower extremes would block the flow completely and create an unreal sealing effect.

The limits for the permeability value are from 0.1 md to 20 Darcy. All the k_h values that were bigger than 20 Darcy were assigned to the 20 Darcy. If the k_h values were smaller than 0.1 md, which is assumed to be the mud permeability, then k_h were reassigned to the lower limit value of 0.1 md.

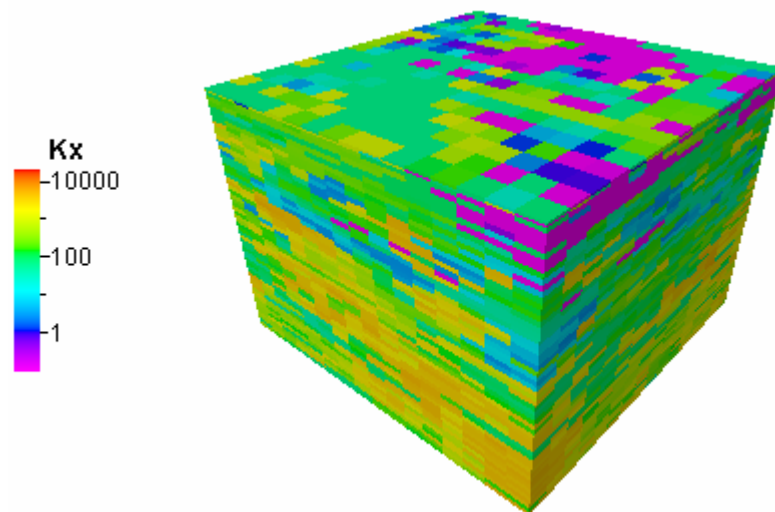
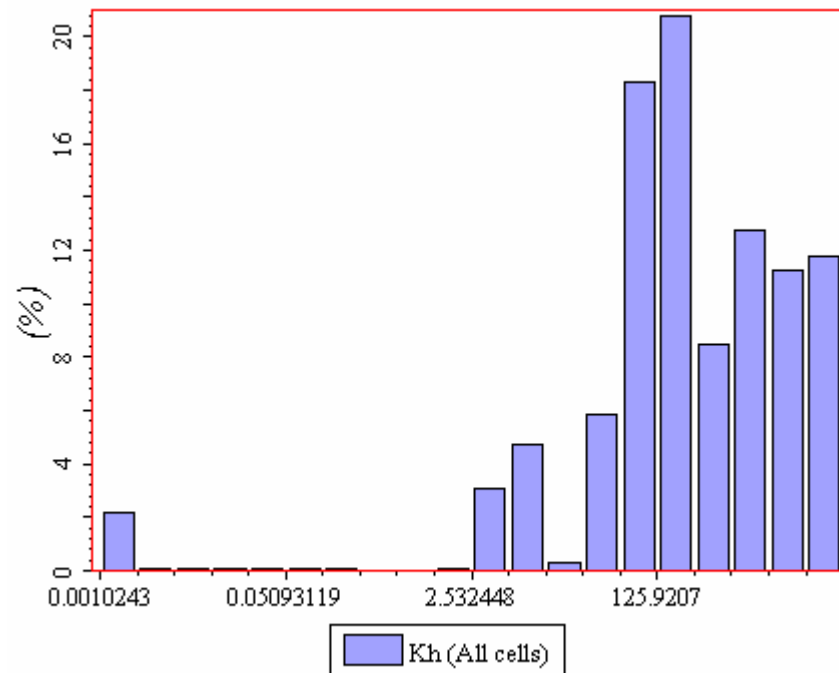


Figure 66: 3D View of calculated k_h on Log Scale



Different power values can be used in a range from -1 to 1 . A value w of 1 corresponds to the arithmetic average, which gives the highest averaged permeability value. A value w of -1 corresponds to the harmonic average, which gives the lowest permeability average. A value w of zero corresponds to the geometric average, which give an averaged value between arithmetic and harmonic averages. Different values of w from one end of 1 to the other end of -1 represent gradual change of flow patterns from flow through parallel layers to cross layer flow. It has been recognized during this study that, for the McMurray system, the power averaging technique is better for estimating the k_v than the harmonic average which is appropriate to use for a flow cross layers.

It was assumed that each cell volume in the reservoir contains two components: one is shale with the permeability of 0.1 md and the other is the reservoir quality component with the permeability of k_h , which was calculated beforehand. The thickness proportion of the two components is the V_{sh} value for this cell. Therefore, the general formula to calculate k_v becomes

$$k_{ave} = \left[V_{sh} k_{mud}^w + (1 - V_{sh}) k_h^w \right]^{\frac{1}{w}} \quad (3)$$

The w value of 0.1 was used in the final calculation of k_v . This value was chosen based on the geological knowledge of the area and confirmed with the satisfactory k_v/k_h ratio.

The result of k_v calculations was then double checked with the k_h values. If k_v is higher than k_h , then was reset to the k_h value. Thus, k_v is always lower than k_h .

A histogram of the calculated vertical permeability is shown in Figure 68. A 3D view of the k_h distribution is shown in Figure 69. A crossplot between k_v and k_h is illustrated in Figure 70. As it is shown, k_v is always smaller than k_h . A 3D distribution of the k_v/k_h ratio is depicted in Figure 71. A crossplot of the k_v/k_h ratio versus V_{sh} is shown in Figure 72. The trend from this crossplot shows a decreasing permeability ratio with increasing V_{sh} values. This trend is geologically acceptable.

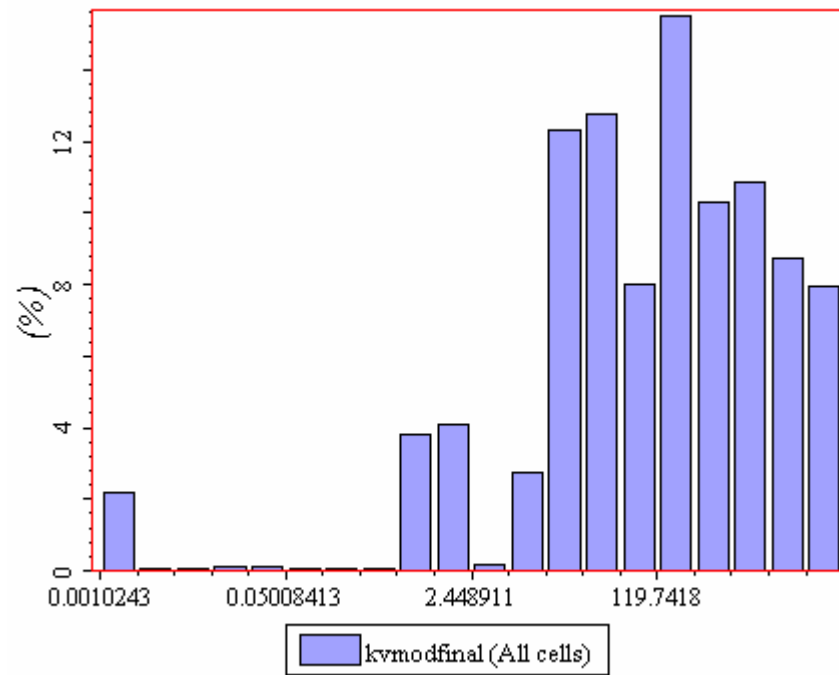


Figure 68: Vertical Permeability

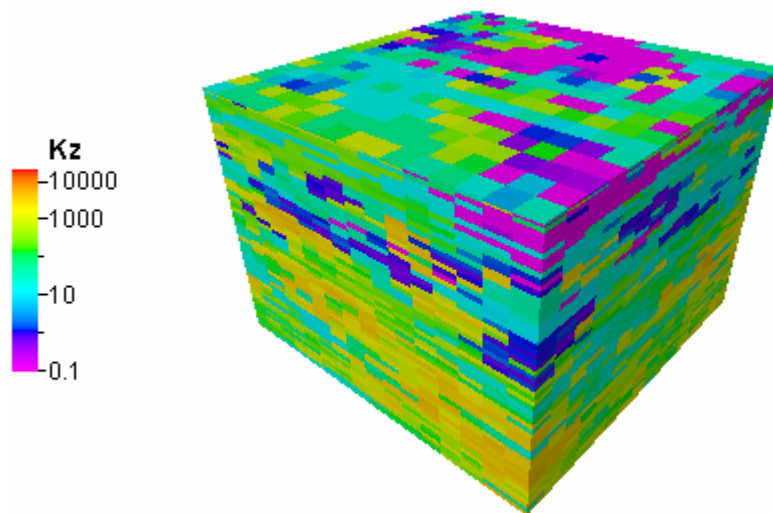


Figure 69: 3D View of calculated k_v on Log Scale

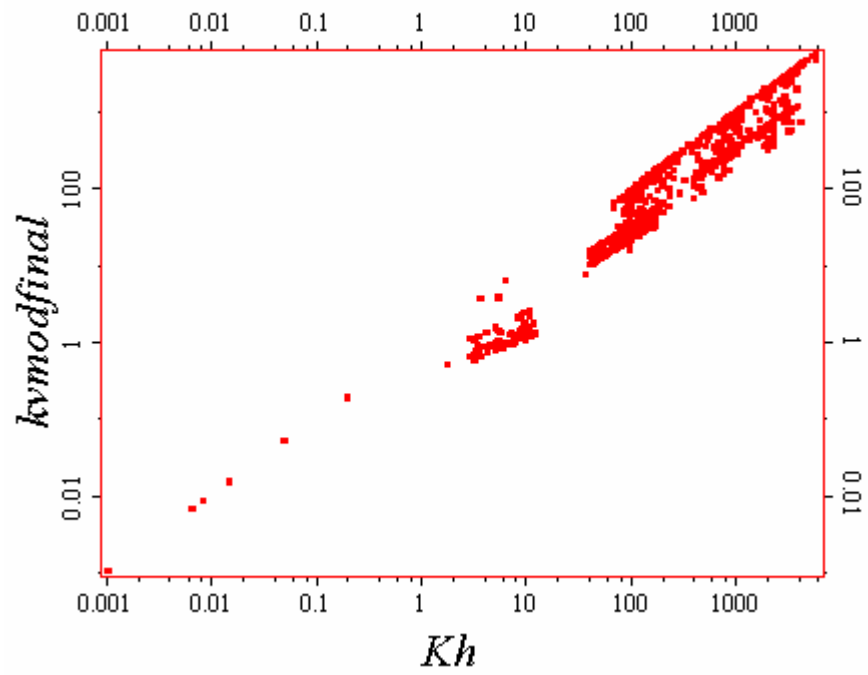


Figure 70: Crossplot of k_v versus k_h on Log Scale

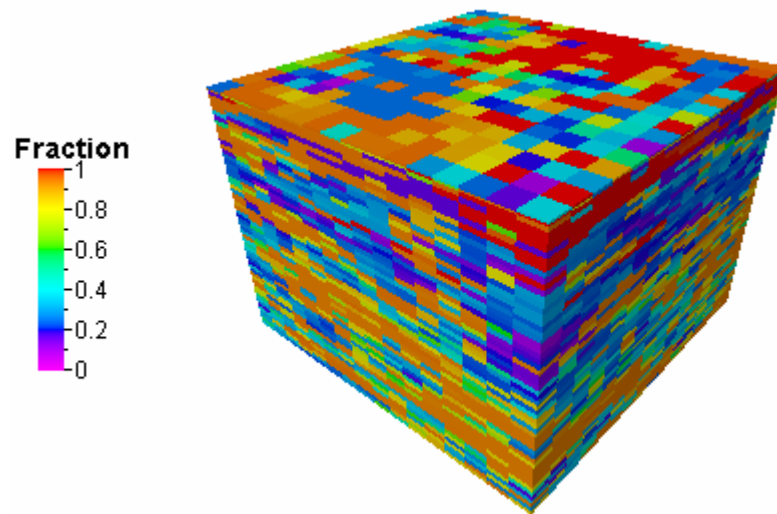


Figure 71: 3D View of k_v/k_h ratio

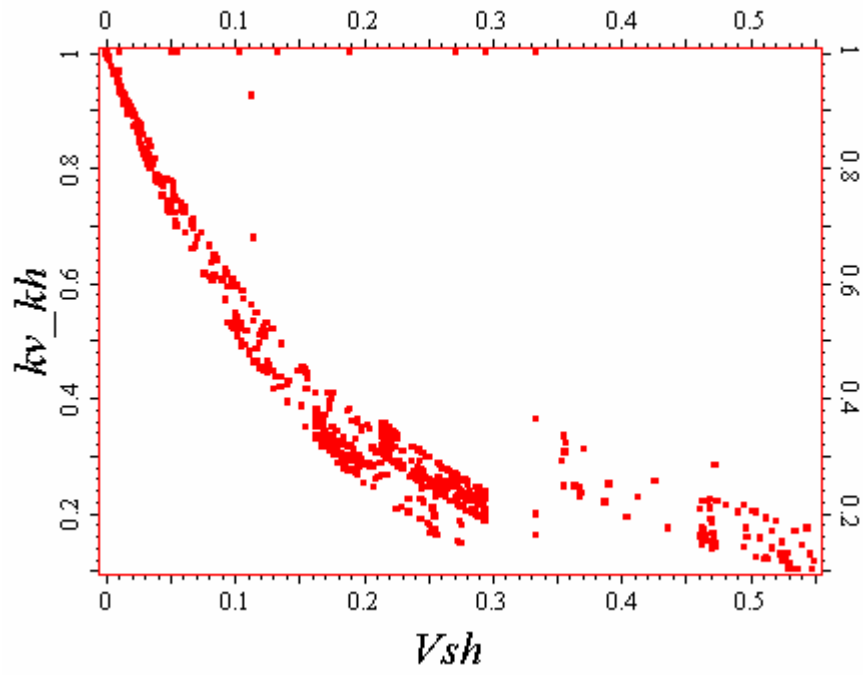


Figure 72: Crossplot of k_v/k_h ratio versus V_{sh}

6. Upscaling for Simulation

The geological grid referenced above was constructed at a flow simulation resolution. Therefore, no upscaling of the current grid was necessary to export to the full pool flow simulation.

6.1. Well-specific Simulation Grid

For SAGD thermal flow simulation, the resolution requirement is much higher than the original 3D geological model in certain direction. Therefore a single well-specific grid was designed to accommodate this grid requirement for thermal simulation.

For better data control of the flow simulation input, the downscaled grid was located at the 12-28 well location. The grid was designed around the 12-28 well path with its long axis oriented at 0° . Figure 73 shows the location and orientation of the grid within the Section 12-28 pool. The downscaled grid is 600m long, 70m wide, and covers the entire McMurray formation in the vertical direction z. It is symmetrical with reference to the well path. The areal view of this grid shows 70 and 12 cells in the x and y directions, respectively. This gridding results in a grid dimension of 1m x 50m x 1m in x, y and z directions, respectively.

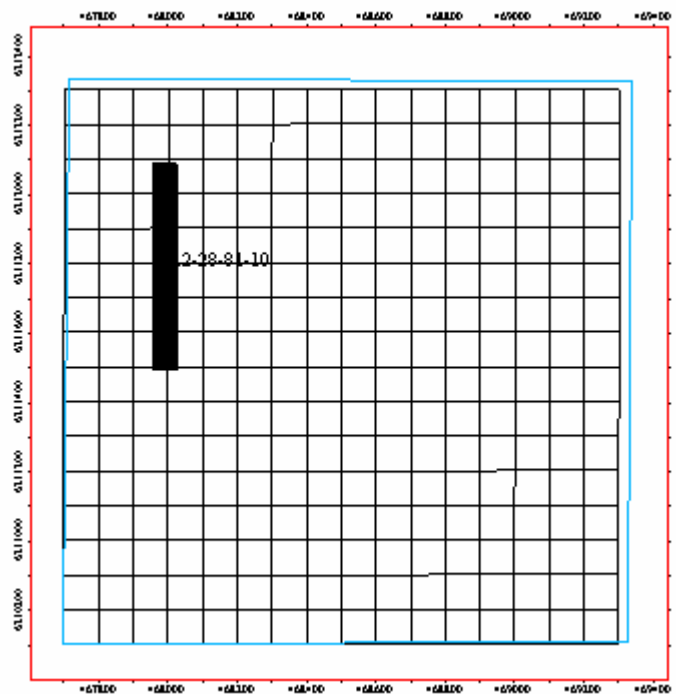


Figure 73: Locations and Orientation of the Downscaled Grids

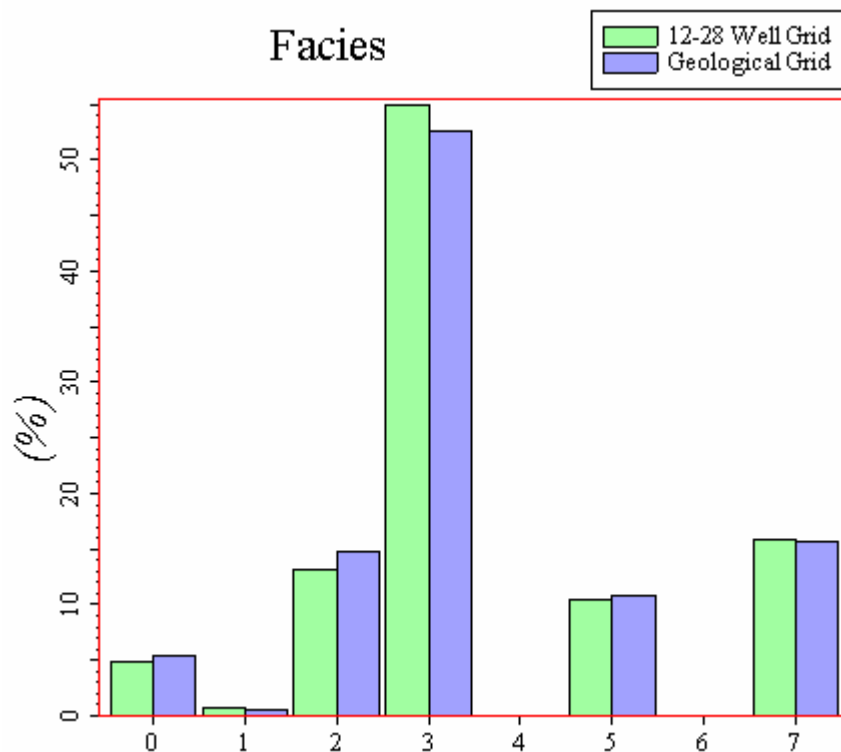
6.2. Upscaling of properties

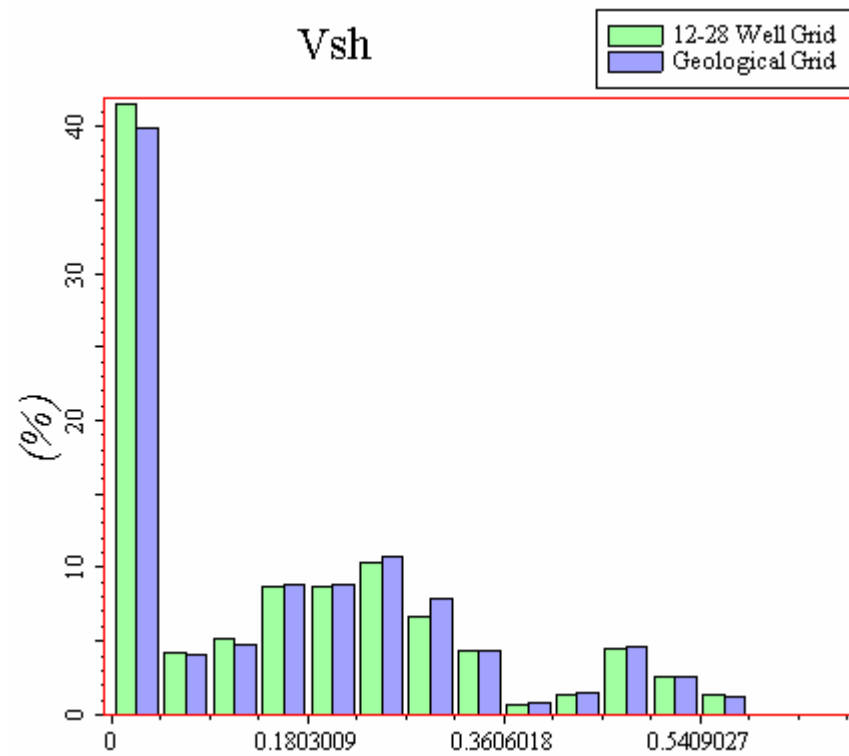
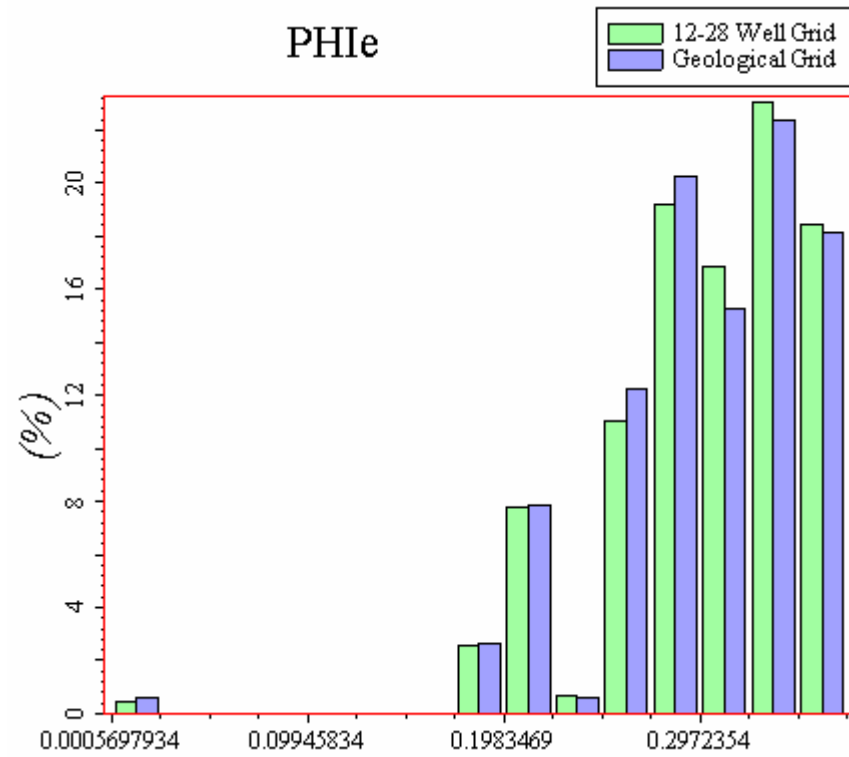
Different averaging methods were used to upscale or downscale properties from the original geological 3D model grid. Facies properties were upscaled using the “Most Of” method, which takes the facies found most frequently in the original 3D finer grid into the coarser flow simulation grid. All other reservoir properties, except the vertical permeability, were upscaled using arithmetic averaging of properties from the original geological grid into the flow simulation grid. This method provided the best match between the cells in the flow simulation grid and the original cells in the geological grid.

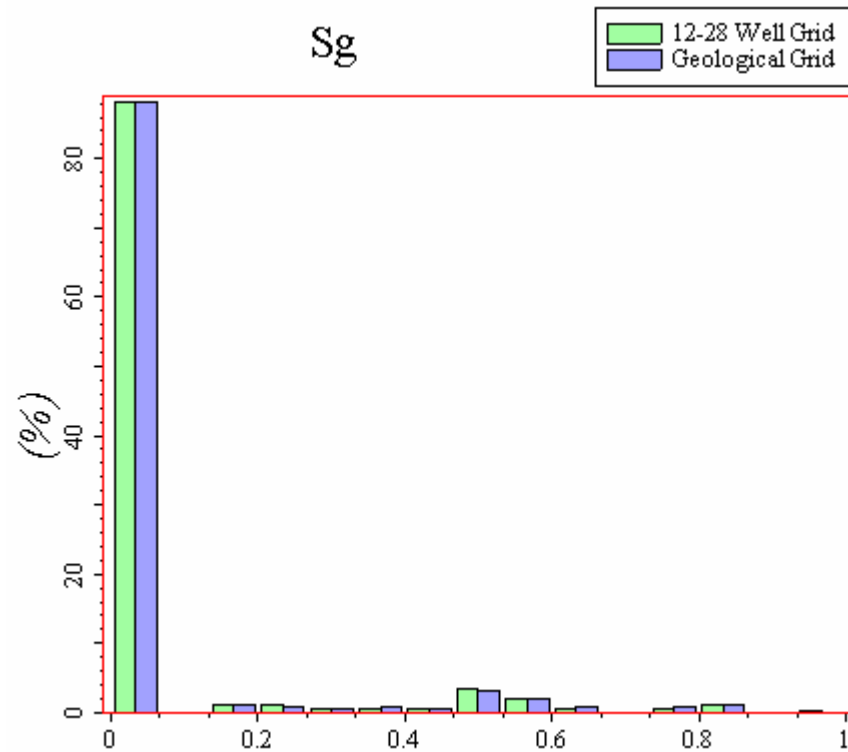
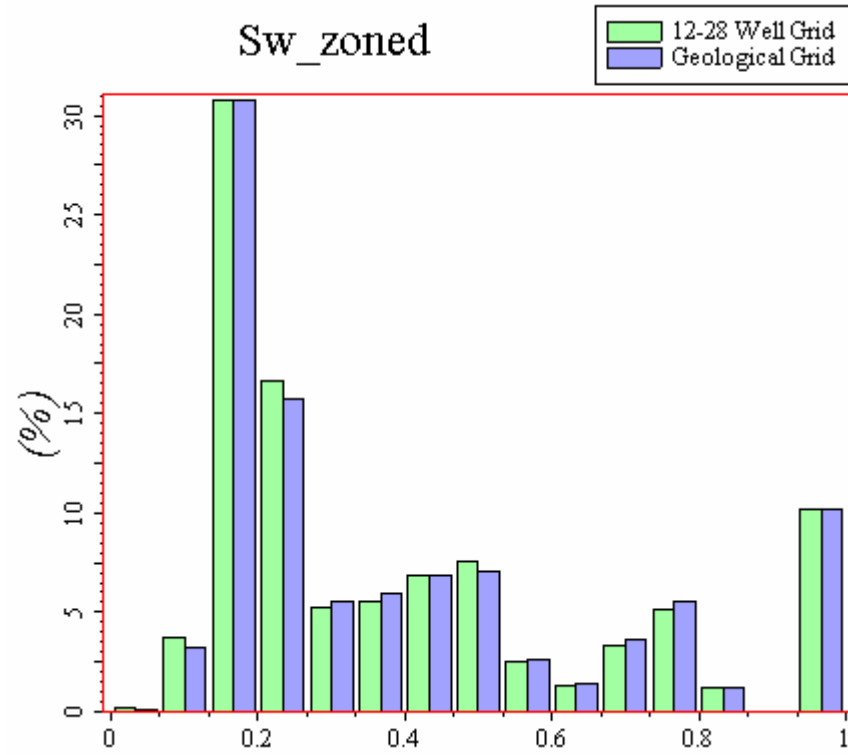
The vertical permeability was recalculated for the flow simulation grid using the power average method (explained in the previous section of this report for vertical permeability calculations), rather than upscaled. The upscaled or downscaled values of k_h and V_{sh} were used to calculate the new values of k_v to ensure that the relationships between permeability, volume of shale, and porosity were correct in each flow simulation grid.

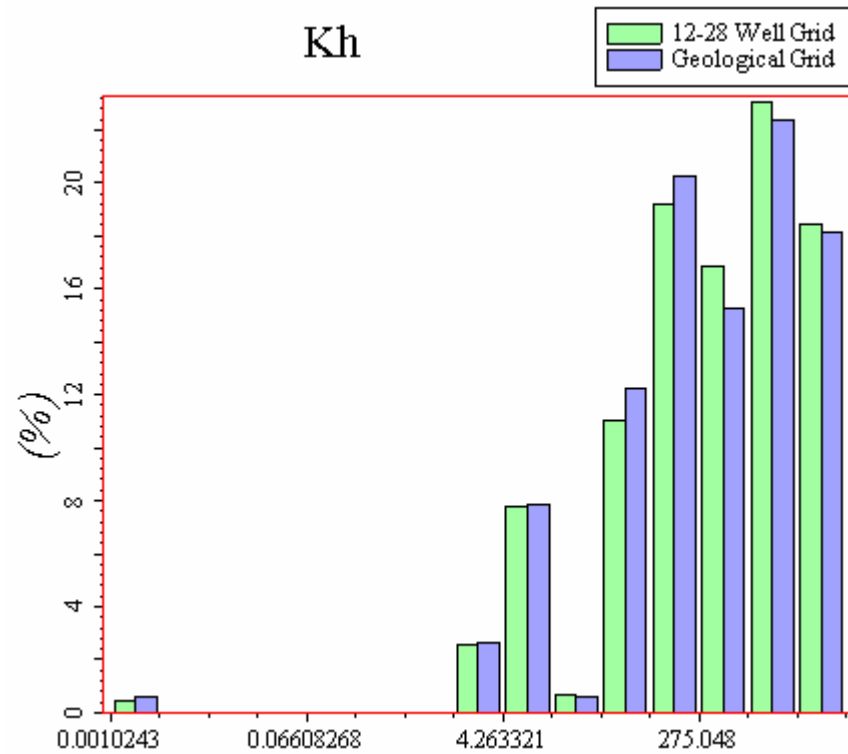
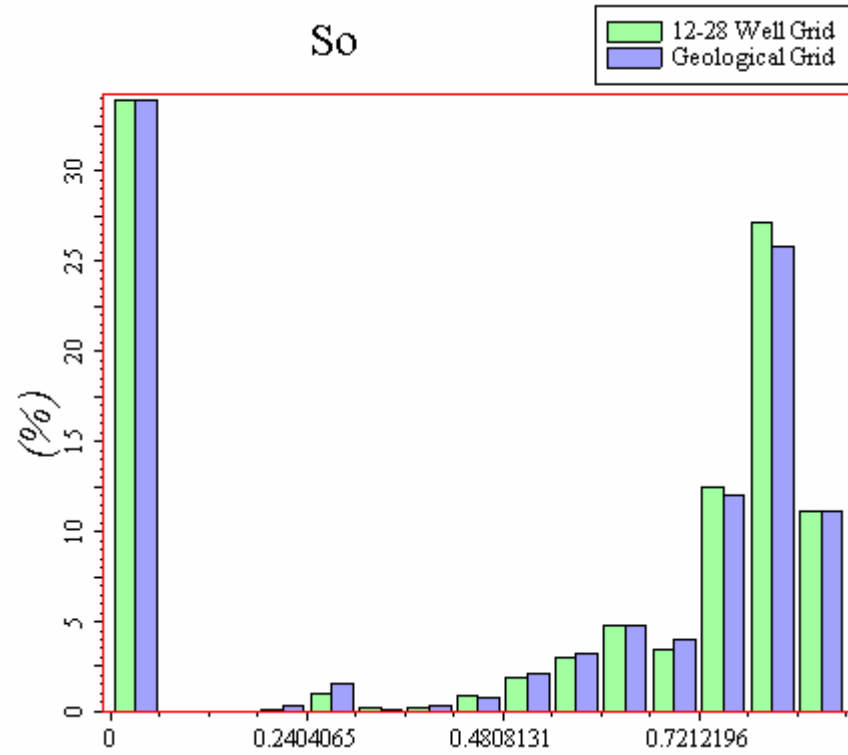
The following histograms describe the relationships between the upscaled and downscaled properties.

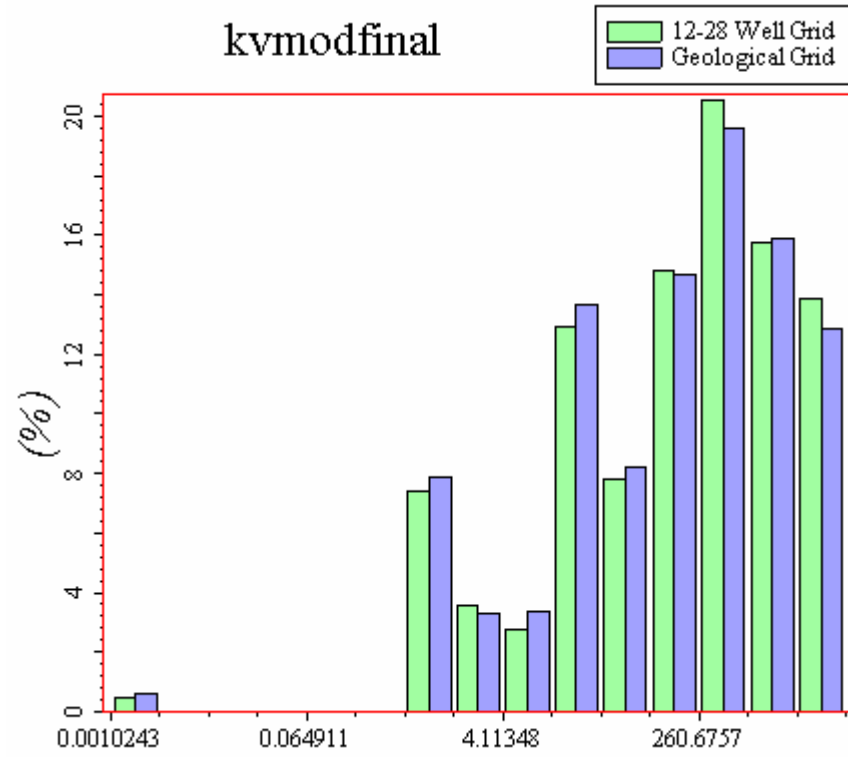
6.2.1. Small Grid Properties











7. Export

7.1. Export format

The chosen grids and their properties were exported using Petrel's grid export functionality. The grids were exported in RESCUE format, version 30, which allows direct import into CMG STARS. The grids were exported with the following properties:

- Facies
 - Porosity
 - Volume of Shale
 - Water Saturation
 - Oil Saturation
 - Gas Saturation
 - Vertical Permeability
 - Horizontal Permeability
-

8. References

1. E. Isaaks and R. Srivastava, An Introduction to Applied Geostatistics, Oxford University Press, New York, 1989.
2. C. Deutsch, MIN E 612: Geostatistical Methods for Modelling Earth Science Data, University of Alberta Course Note, 1998.
3. C. Deutsch and A. Journel, GSLIB: Geostatistical Software Library and User's Guide, Second Edition, Oxford University Press, New York, NW, 1997.
4. Log Analysis Report Basal Wabiscaw/McMurray Sandstones Hangingstone McMurray X Pool, Alberta, Ross Crain, 1st November 2004, Confidential Report Prepared for Paramount Energy Trust Ltd.
5. H. Nguyen, Master Thesis, University of Alberta, Canada, 2001